

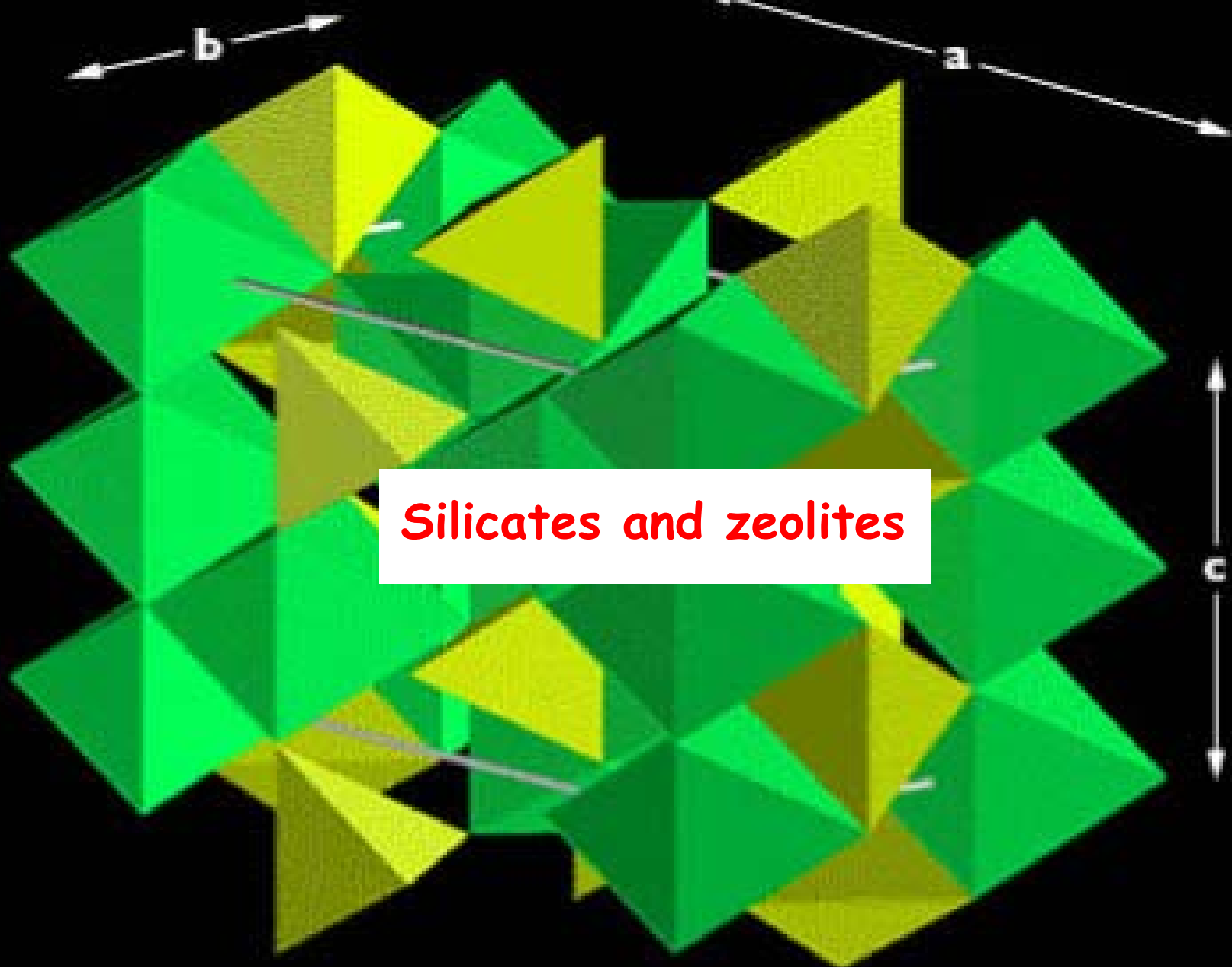
Zeolites and porous materials: synthesis and applications



UE LS 205

C. Bonhomme, Professor

Université P. et M. Curie, Paris 6



Silicates and zeolites

 Mg^{2+}, Fe^{2+}

 Si

Silicates

wt. % in earth crust:

O: 47 %

Si: 28 %

Al: 5 %

Fe: 5 %

Ca: 3.5 %

Na: 2.8 %

K: 2.6 %

Mg: 2 %

.....

silicates and
aluminosilicates

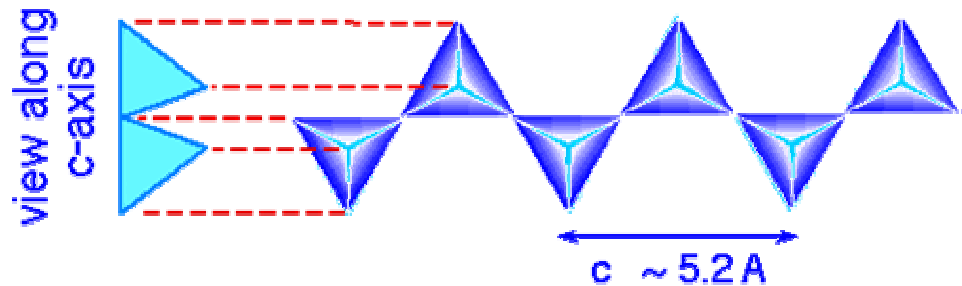
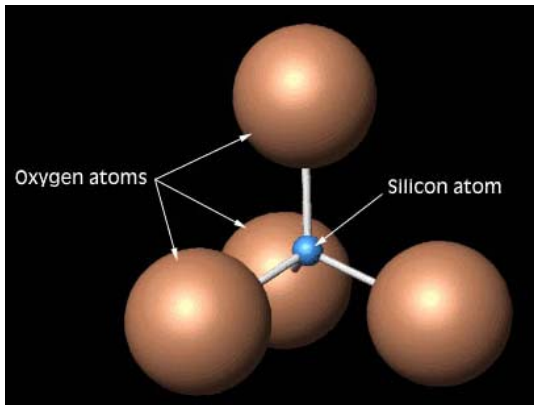
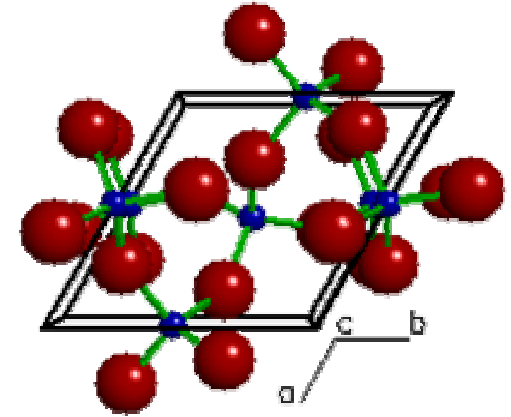
$$\chi(\text{Al}) \sim \chi(\text{Si})$$

$$r(\text{Al}^{3+})/r(\text{O}^{2-}) \sim 0.43$$

$$\text{CN}(\text{Al}): 4 \text{ or } 6!$$

but... a very large variety of structures!...

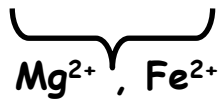
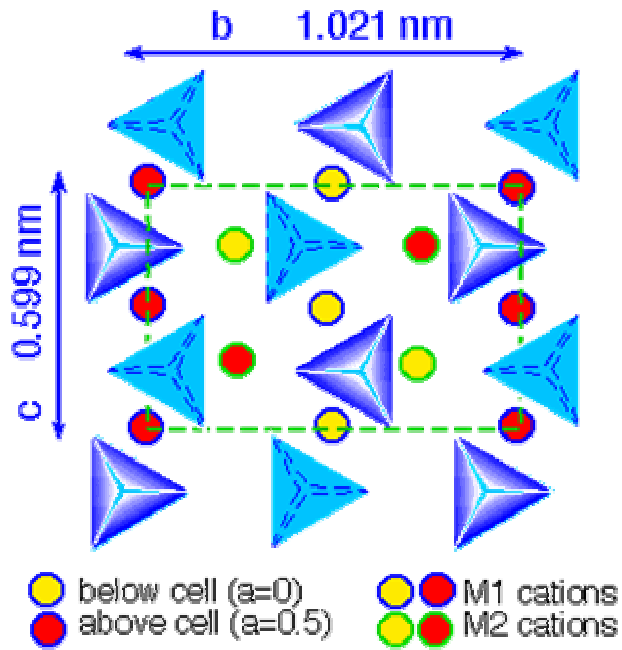
NESOSILICATES
SOROSILICATES
CYCLOSILICATES
INOSILICATES
PHYLLOSILICATES
TECTOSILICATES



the basic structural unit: SiO_4^{4-}  linked by vertices (only...)

Neso- and sorosilicates

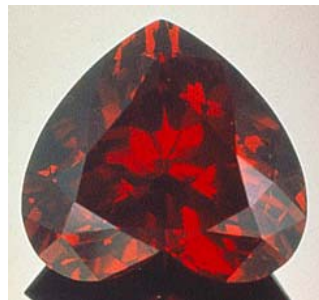
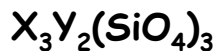
«isolated» SiO_4^{4-} units: nesosilicates



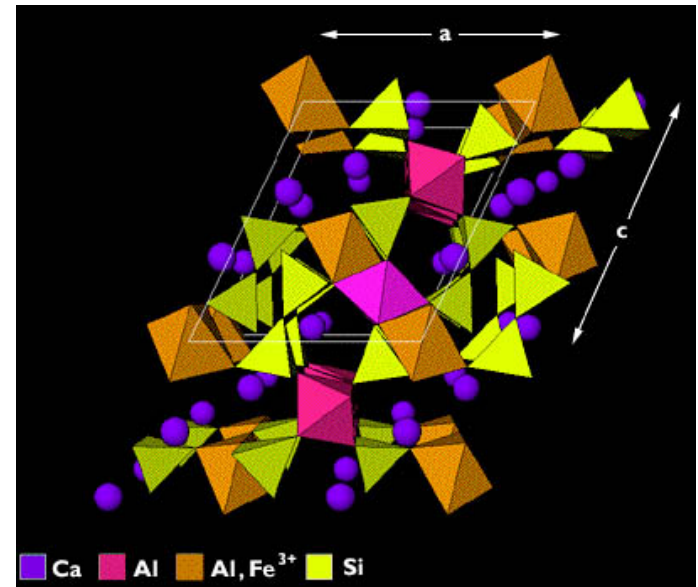
Mg_2SiO_4 : Forsterite

$(\text{Mg}, \text{Fe})_2\text{SiO}_4$: Olivine

other examples: garnets,
Portland cement...



«isolated» $\text{Si}_2\text{O}_7^{6-}$ units: sorosilicates



$\text{Sc}_2(\text{Si}_2\text{O}_7)$: Thortveitite

$\text{Zn}_4(\text{Si}_2\text{O}_7)(\text{OH})_2, \text{H}_2\text{O}$: Hemimorphite

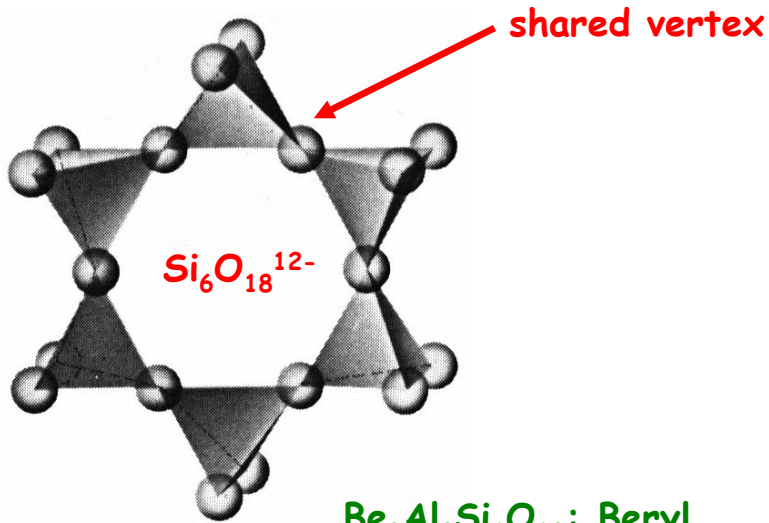
other units (rare!): $\text{Si}_3\text{O}_{10}^{8-}$, $\text{Si}_4\text{O}_{13}^{10-}$

$\text{SiO}_2, \text{Ag}_2\text{O}, T \sim 600^\circ\text{C}, P(\text{O}_2) \sim 4.5 \text{ kBar}$

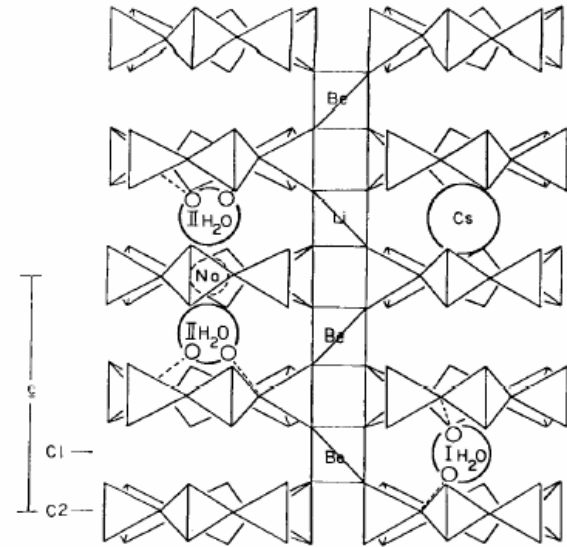


Cyclosilicates

Cycles including 3, 4, 6 or 8 silicate units: $(\text{Si}_n\text{O}_{3n})^{2n-}$ ($n = 3, 4, 6, 8$)

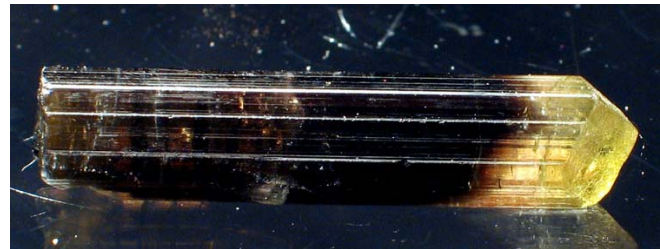


$\text{Be}_3\text{Al}_2\text{Si}_6\text{O}_{18}$: Beryl
or...emerald!



High-temperature structure and crystal chemistry of hydrous alkali-rich beryl from the Harding pegmatite, Taos County, New Mexico

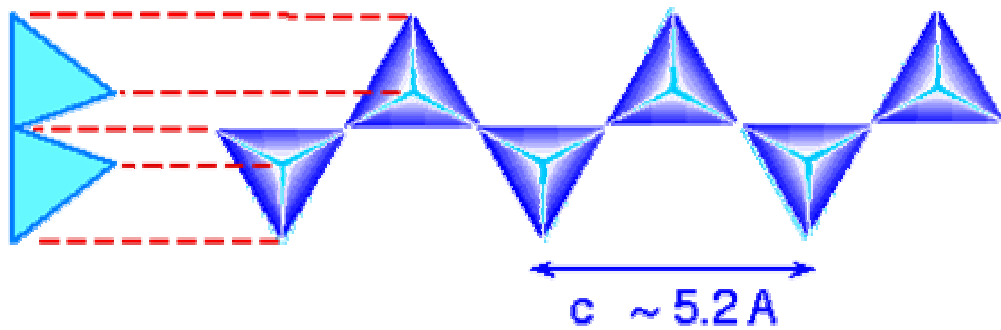
GORDON E. BROWN, JR., BRADFORD A. MILLS¹
Department of Geology, Stanford University, Stanford, California 94305



$(\text{Na}, \text{Ca})(\text{Li}, \text{Mg}, \text{Al})_3(\text{Al}, \text{Fe}, \text{Mn})_6(\text{OH})_4(\text{BO}_3)_3\text{Si}_6\text{O}_{18}$: Tourmaline 5

Inosilicates

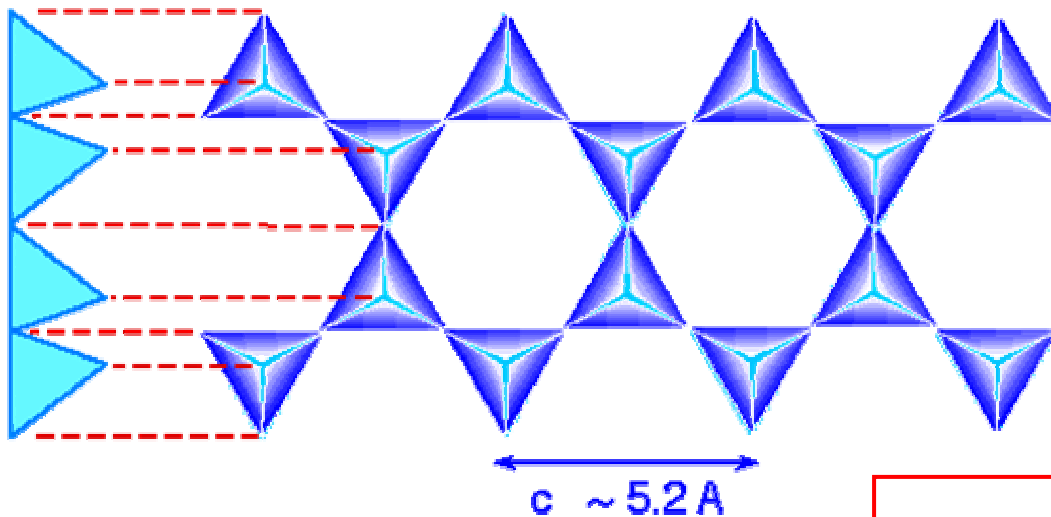
view along
c-axis



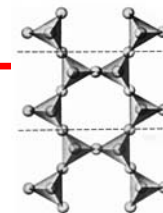
pyroxenes



view along
c-axis



amphiboles



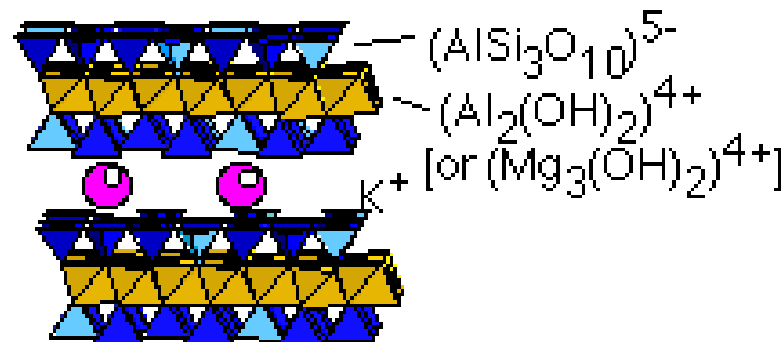
properties of fibers

Phyllosilicates

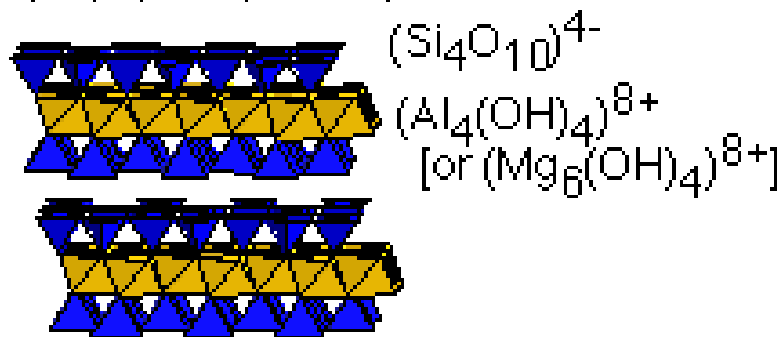
Kaolinite (or Antigorite)



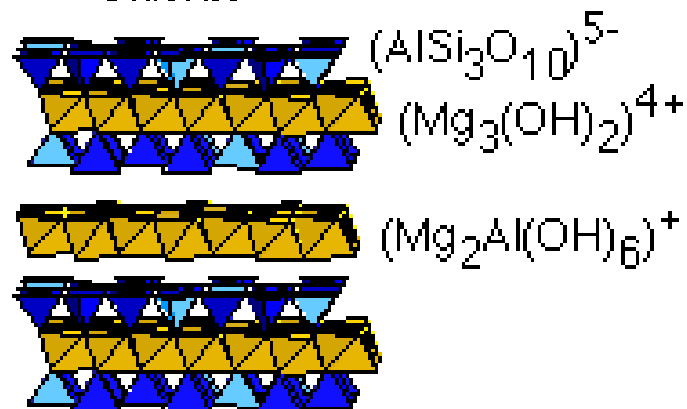
Muscovite (or Biotite)



Pyrophyllite (or Talc)



Chlorite



but also...clays! (intercalation of water molecules)
(montmorillonite...)

plastic properties

Tectosilicates



silica

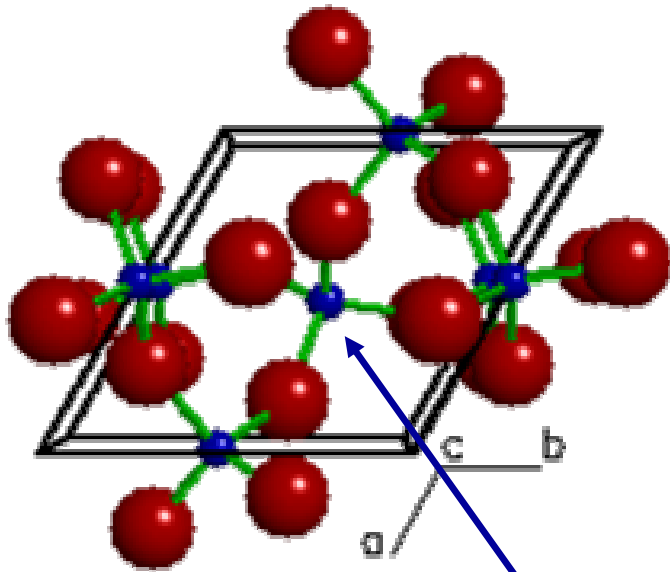
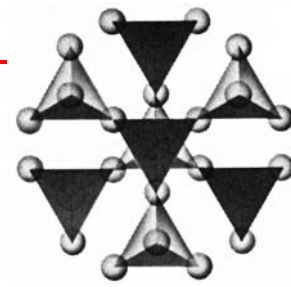
Feldspaths

zeolites

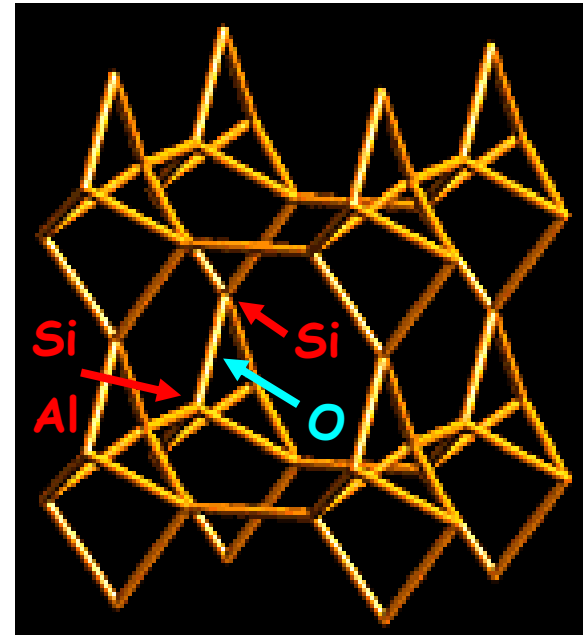
} porosity?



Feldspath (plagioclase)



Si



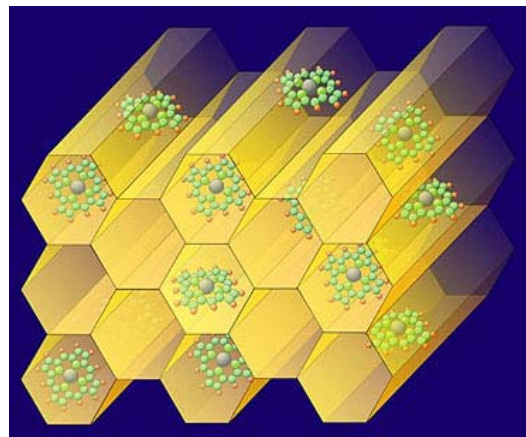
a typical zeolite structure

porous materials

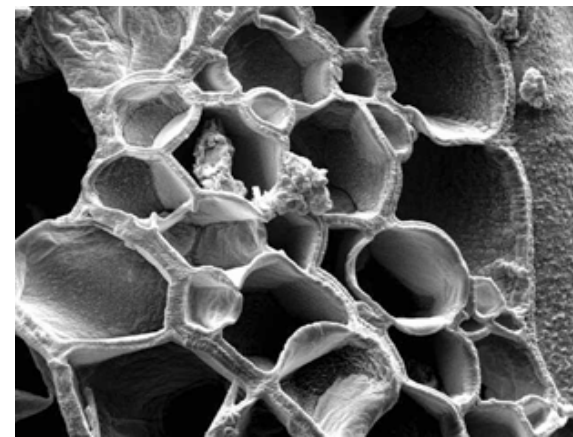
nanoporous
 $\emptyset < 2 \text{ nm}$

mesoporous
 $2 < \emptyset < 50 \text{ nm}$

macroporous
 $50 \text{ nm} < \emptyset$



MCM



foams

Zeolites

discovered by Baron A. Von Kronstedt

ZEO: to boil
LITHOS: stone

(1756)

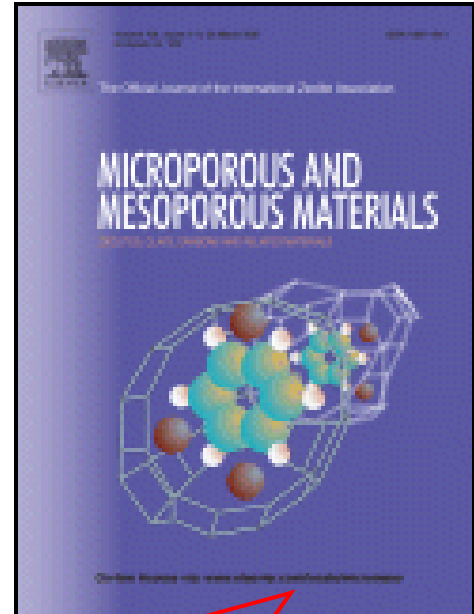


characteristics...

- exchangeable cations
(neutrality)



- rigid anionic networks
- cavities and channels
- guest molecules (water...)

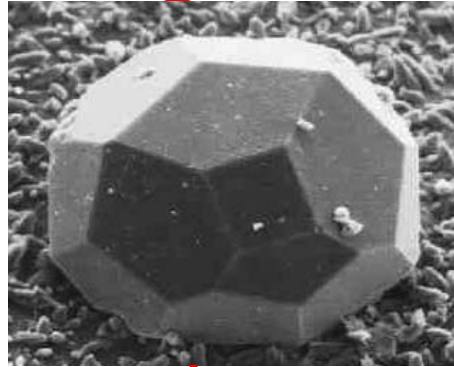


official journal of the
international zeolite association

Natural zeolites



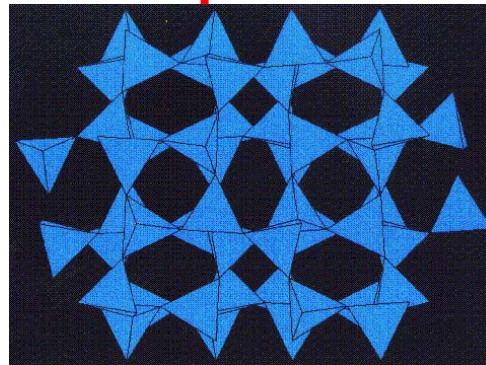
~ 40 natural zeolites



Natrolite



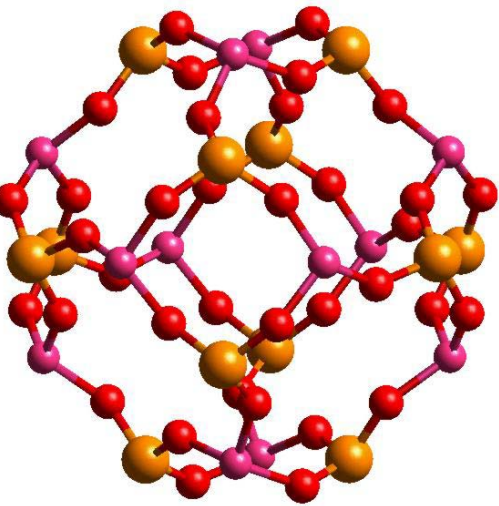
Faujasite



Anacilme

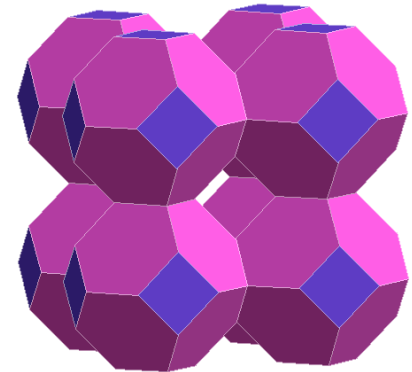
The sodalite cage

Sodalite, a mineral: $\text{Na}_8\text{Al}_6\text{Si}_6\text{O}_{24}\text{Cl}_2$



the sodalite entity

24 linked tetrahedra
(Si or Al)

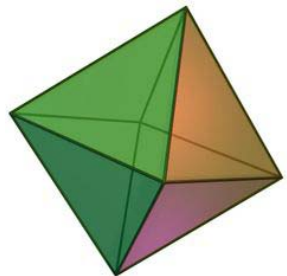


Sodalite (mineral)

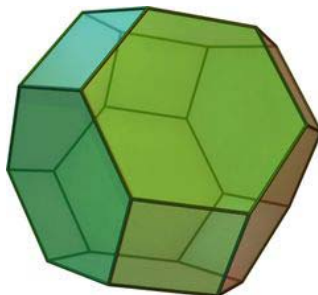
Lapis-lazuli



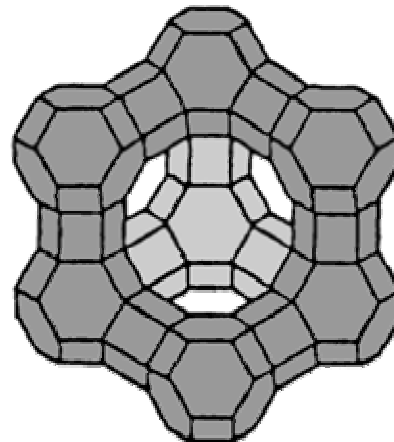
Linde-A (synthetic)



octahedron



truncated octahedron



Faujasite (mineral)

$\text{NaCa}_{1.5}(\text{Al}_2\text{Si}_5\text{O}_{14}) \cdot 10\text{H}_2\text{O}$

Some characteristics of zeolites

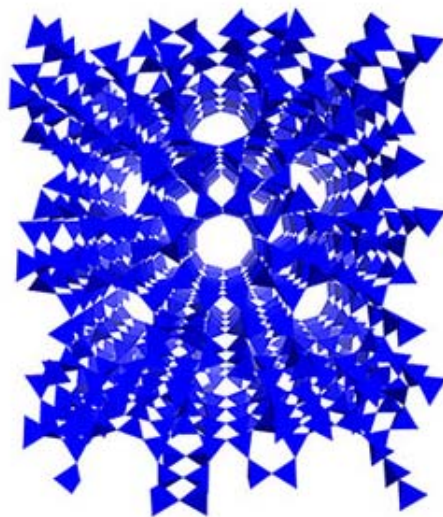
A- the Si/Al ratio

Linde-A: Si/Al = 1

Mordenite (mineral): Si/Al = 5.5

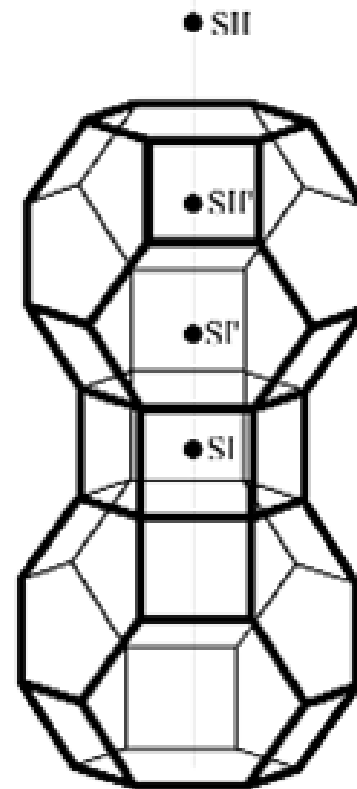
ZSM: $20 < \text{Si/Al} < \infty!$ (hydrophobic)

C- cavities and tunnels



B- exchangeable cations

various accessible sites



Zeolithe

tetrahedra

Ø (pm)

Sodalite

4

260

Linde-A

8

410

ZSM-5

10

510×560

Faujasite

12

740

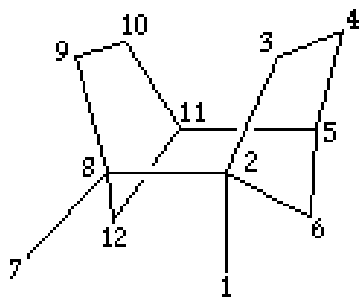
Mordenite

12

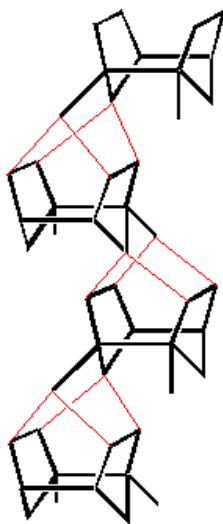
670×700

Synthetic zeolites: the ZSM family

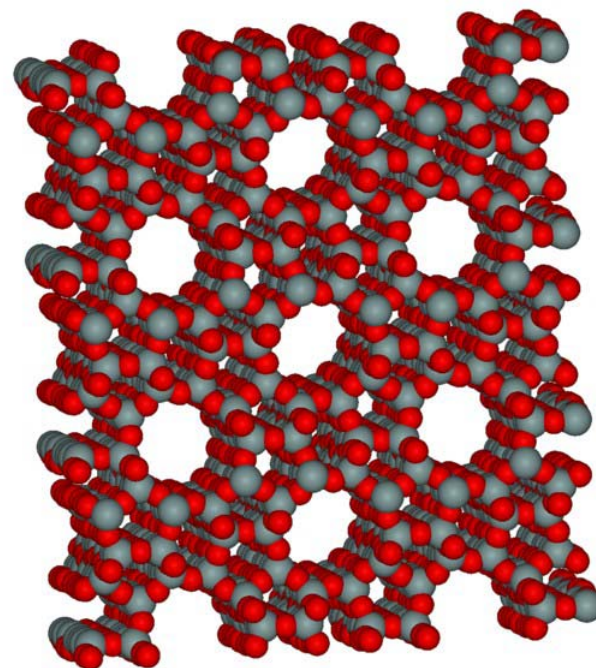
Zeolite Socony Mobil (~ 1975)



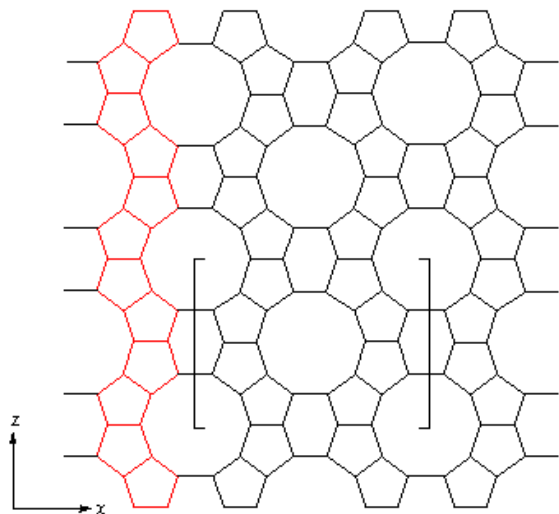
«Pentasil» unit
(five-membered rings)



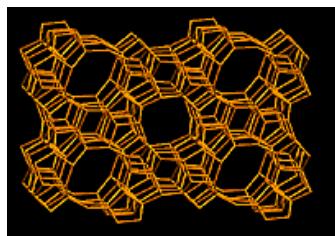
chains



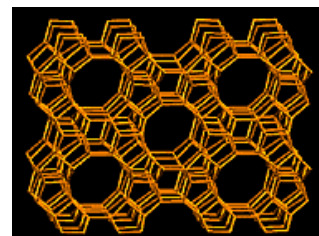
3D architecture ZSM-5



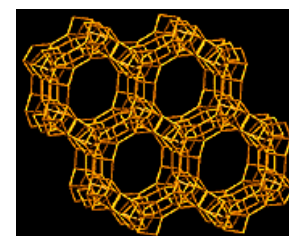
planes



ZSM-5

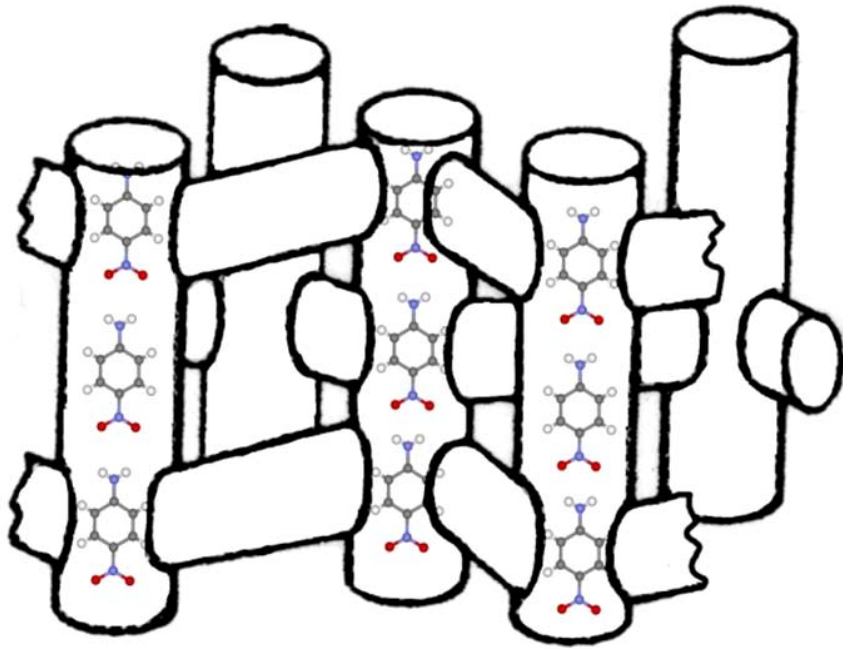


ZSM-11

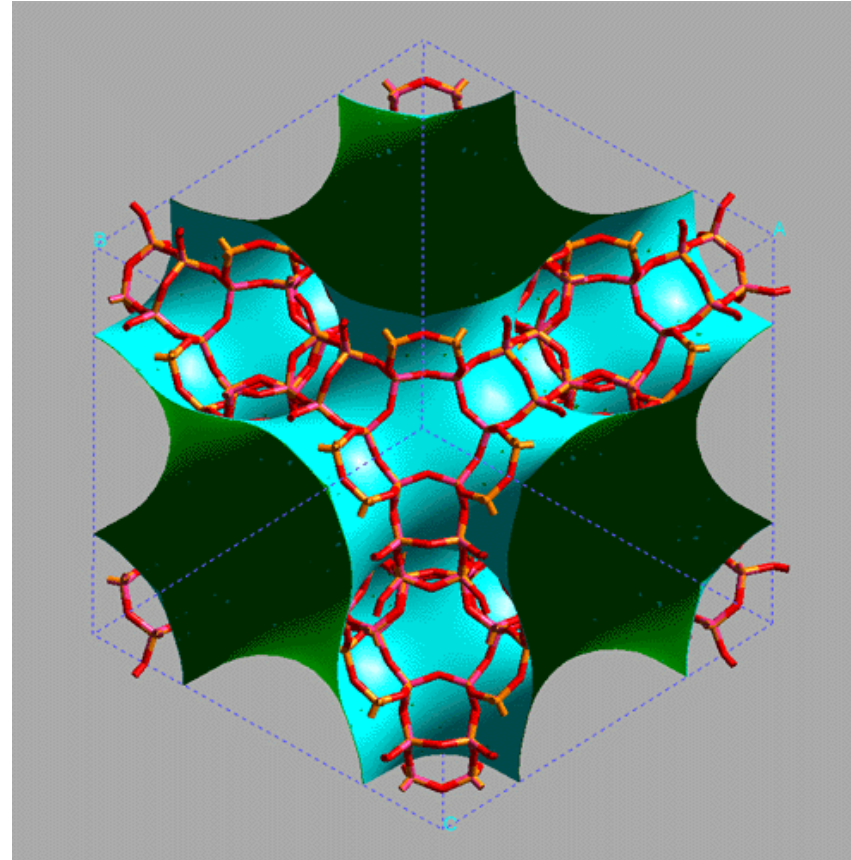


ZSM-18

Interconnected channels: structural dependence

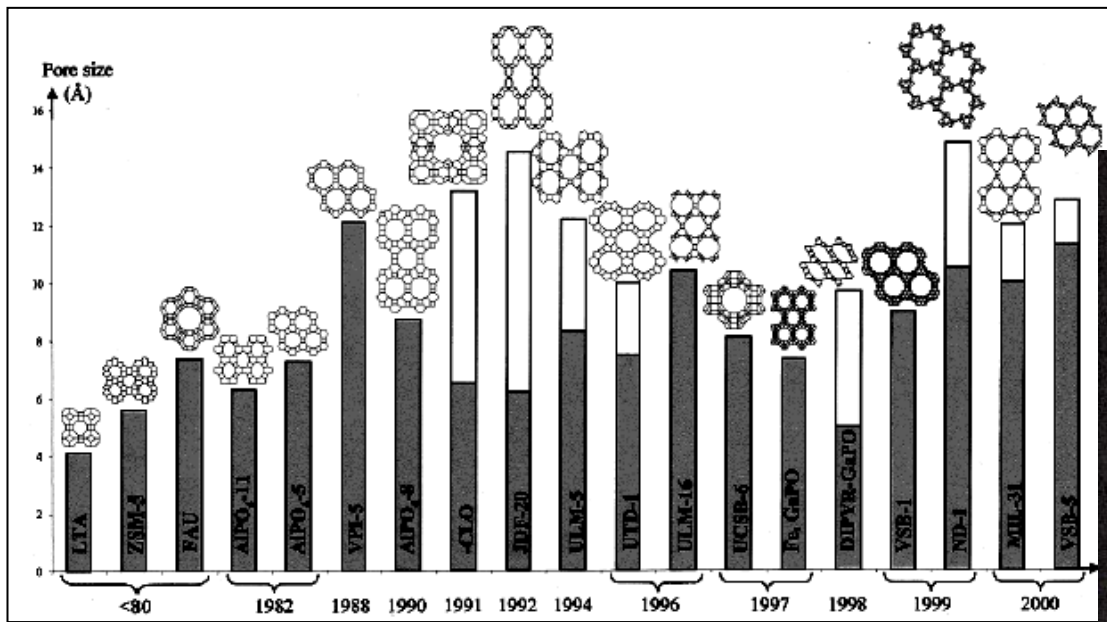


ZSM-5

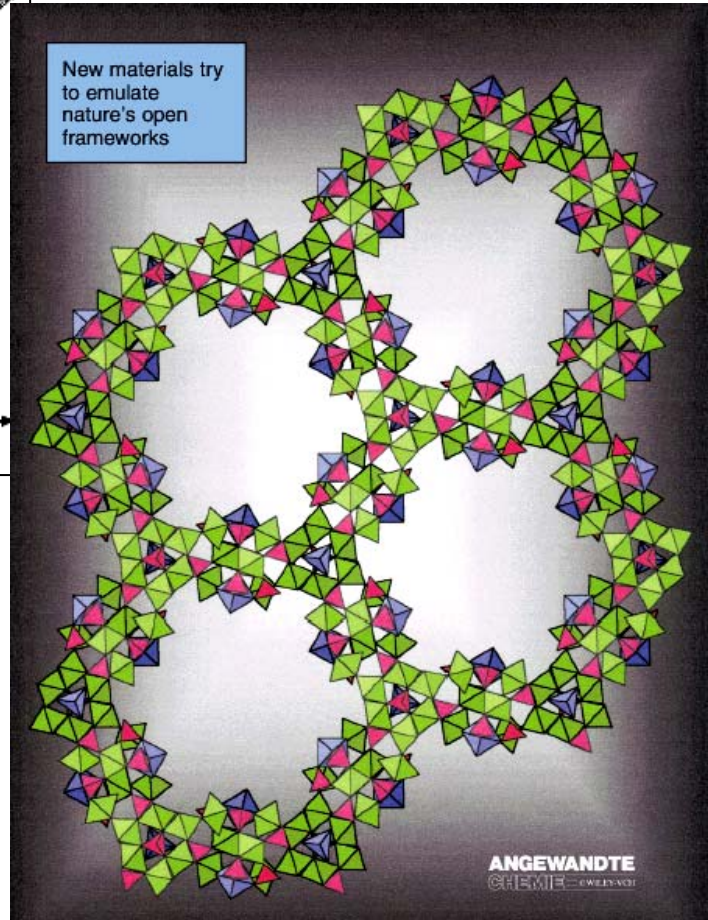


Faujasite

More and more porosity!



New materials try to emulate nature's open frameworks



~ 200 synthetic zeolites!

ANGEWANDTE
CHEMIE

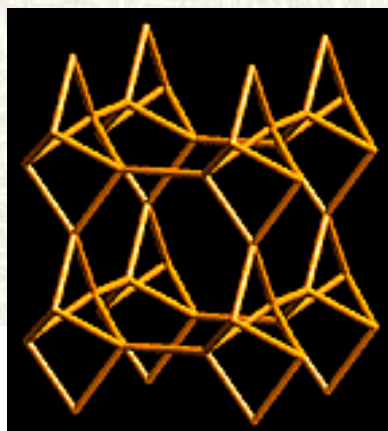
Zeolite Type Categories and Framework Type Groups

Zeolite type categories

- Silicates
- Phosphates

Framework type groups

- Silicates
- Phosphates
- Both, silicates and phosphates



EDI

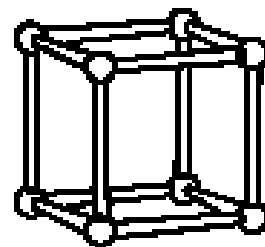
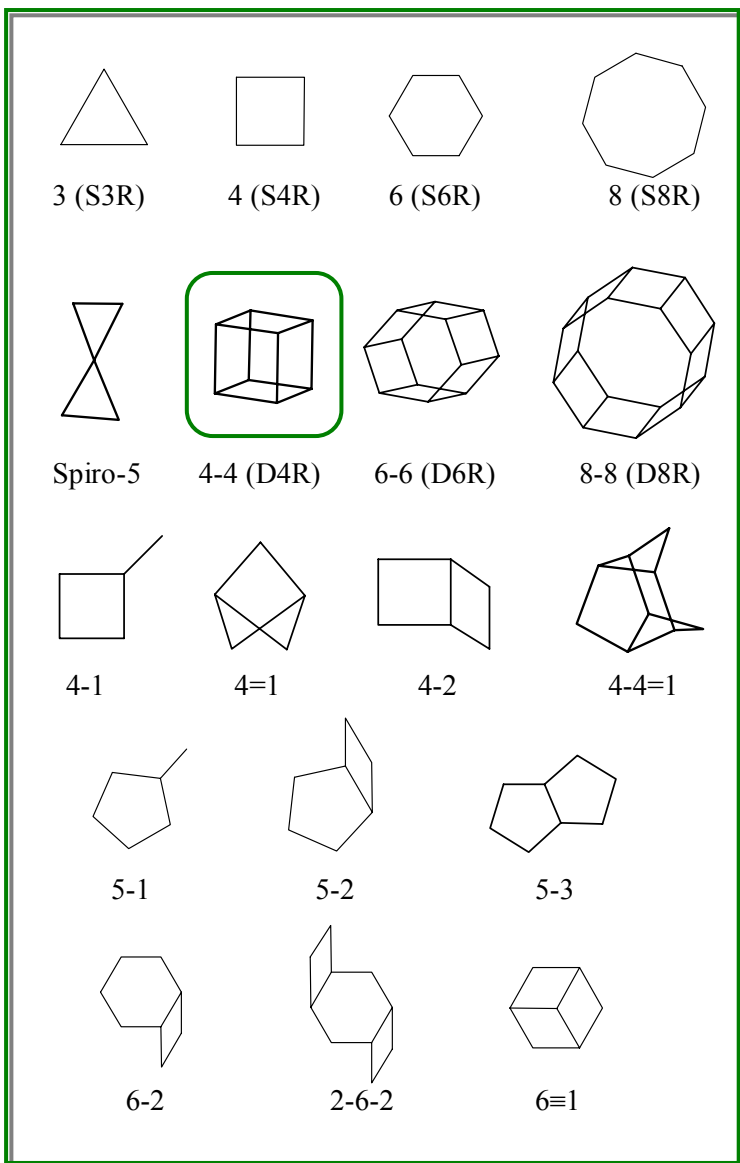
Si

(Si,P)

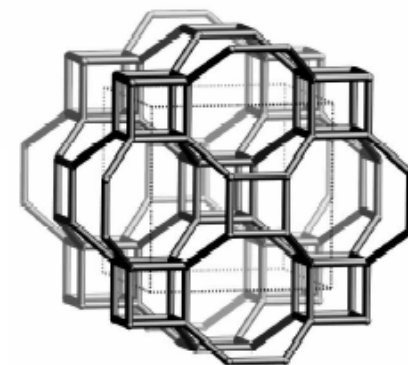
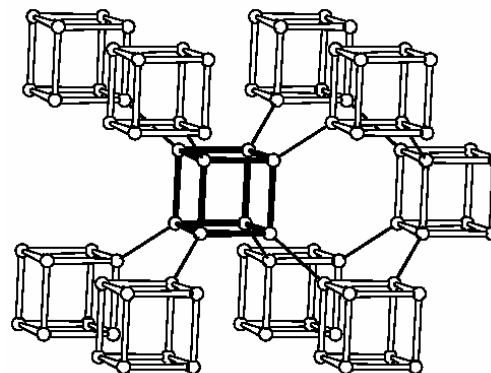
P

Silicates ^a			Both Silicates and Phosphates	Phosphates ^b	
AFG	IFR	OFF	ABW	ACO	SAO
ASV	ISV	OSO	AET	AEI	SAS
*BEA	ITE	-PAR	AFI	AEL	SAT
BIK	JBW	PAU	AFX	AEN	SAV
BOG	KFI	-RON	ANA	AFN	SBE
BRE	LIO	RSN	AST	AFO	SBS
CAS	LOV	RTE	BPH	AFR	SBT
CFI	LTN	RTH	CAN	AFS	VF1
-CHI	MAZ	RUT	CGS	AFT	WEI
CON	MEI	SFE	CHA	AFY	ZON
DAC	MEL	SFF	DFT	AHT	
DDR	MEP	SGT	EDI	APC	
DOH	MFI	STF	ERI	APD	
DON	MFS	STI	FAU	ATN	
EAB	MON	STT	GIS	ATO	
EMT	MOR	TER	LAU	ATS	
EPI	MSO	TON	LEV	ATT	
ESV	MTF	TSC	LOS	ATV	
EUO	MTN	VET	LTA	AWO	
FER	MTT	VNI	LTL	AWW	
FRA	MTW	VSV	MER	CGF	
GME	MWW	-WEN	PHI	-CLO	
GON	NAT	YUG	RHO	CZP	
GOO	NES		SOD	DFO	
HEU	NON		THO	OSI	

Secondary Building Units (SBU)

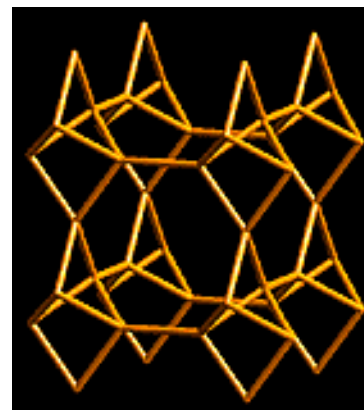
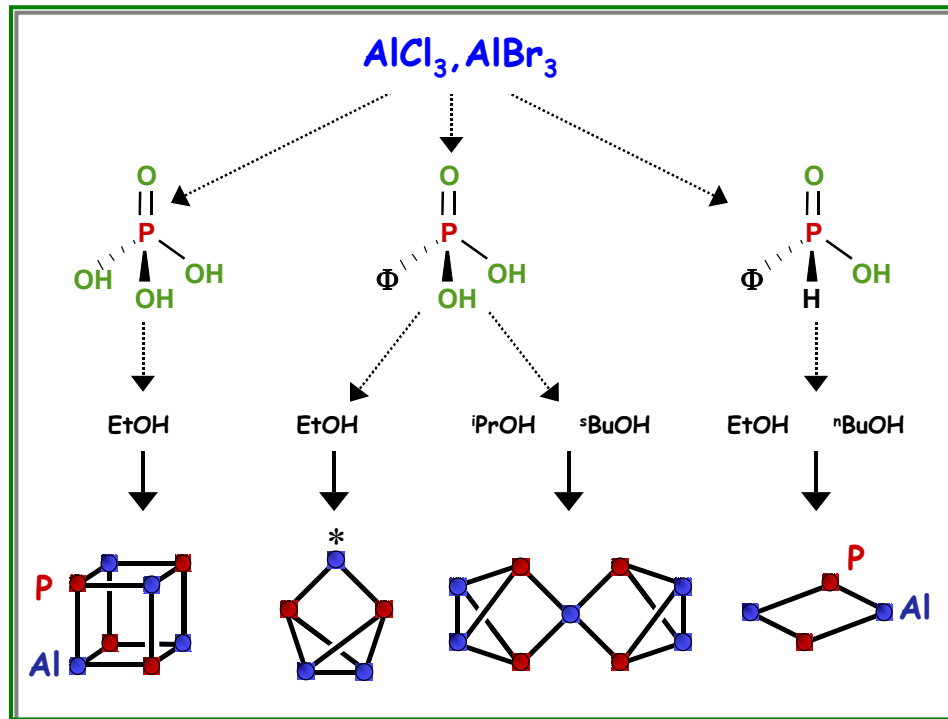
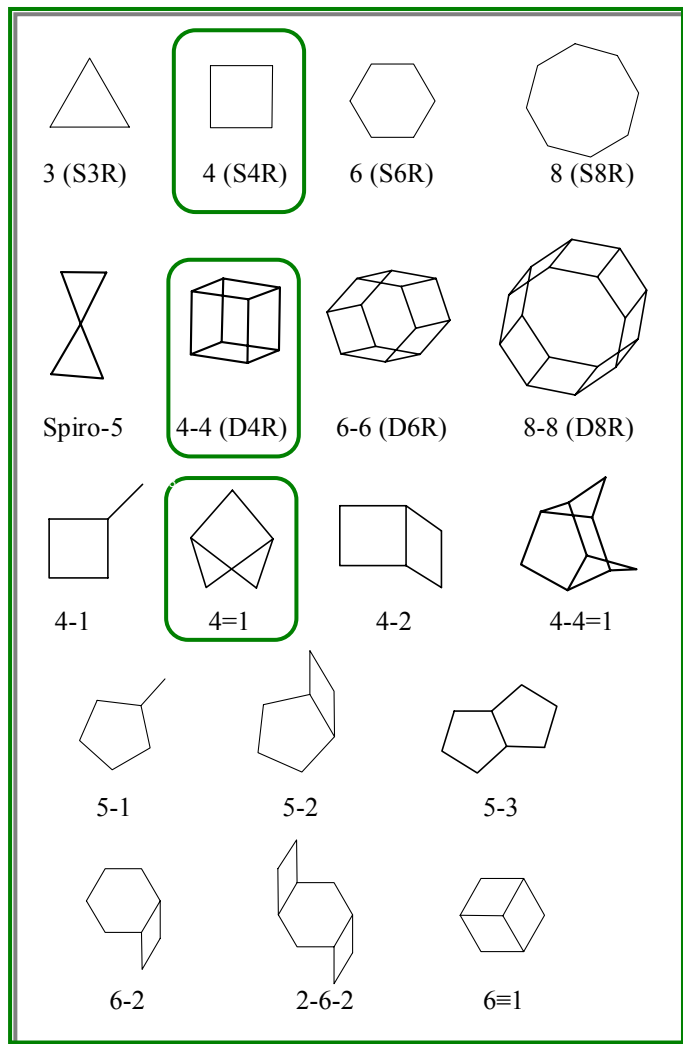


D4R type SBU



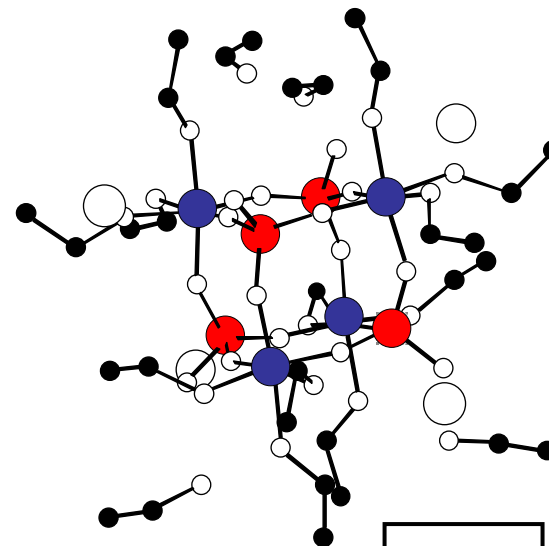
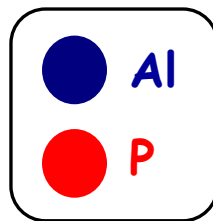
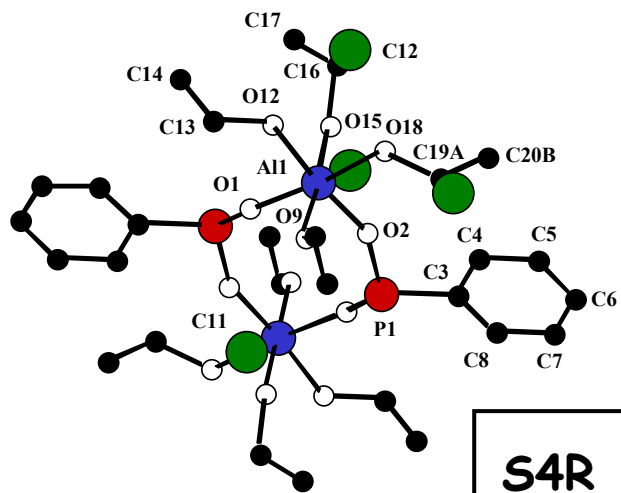
ACO type

T. Azais

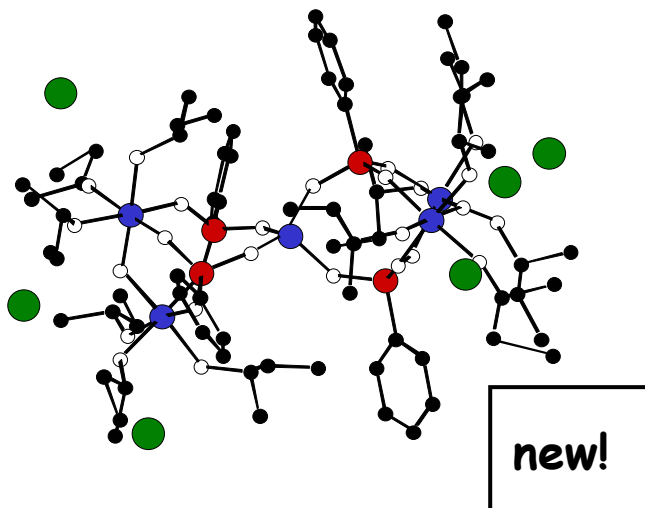


EDI type

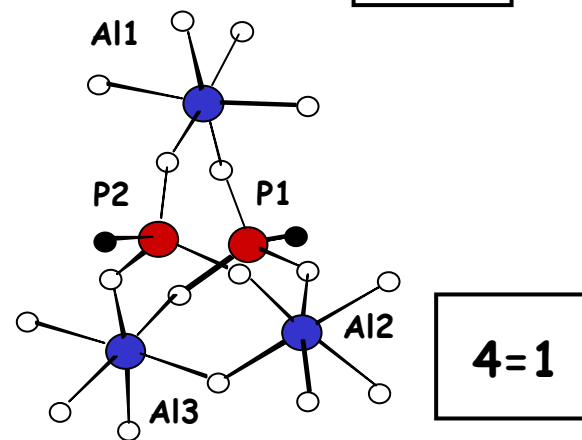
Cluster structures



D4R

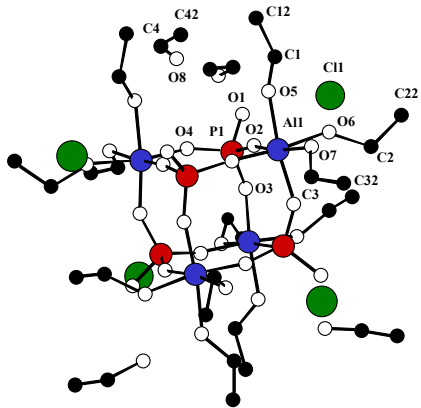


new!

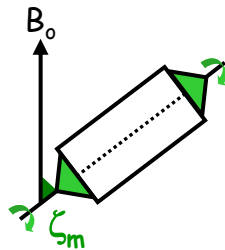
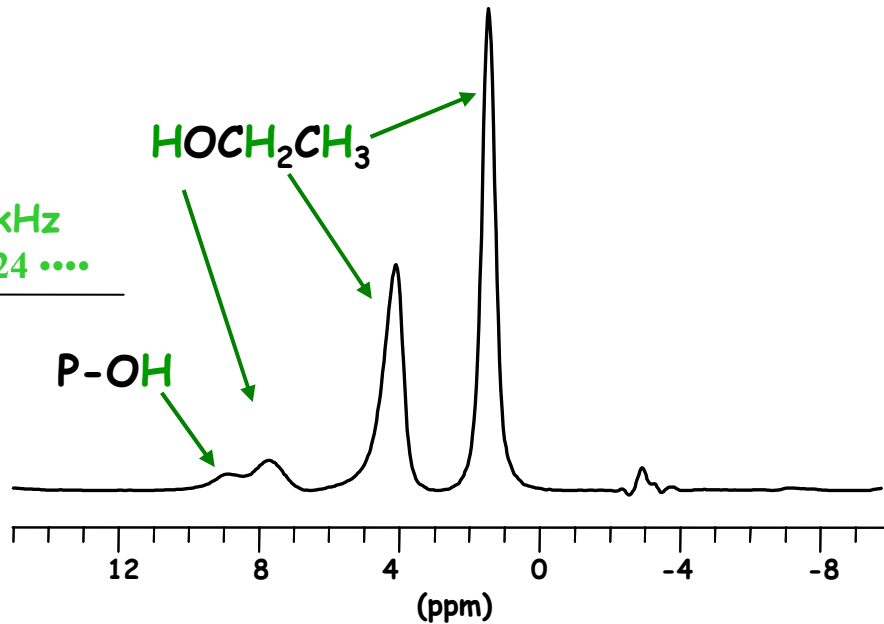


4=1

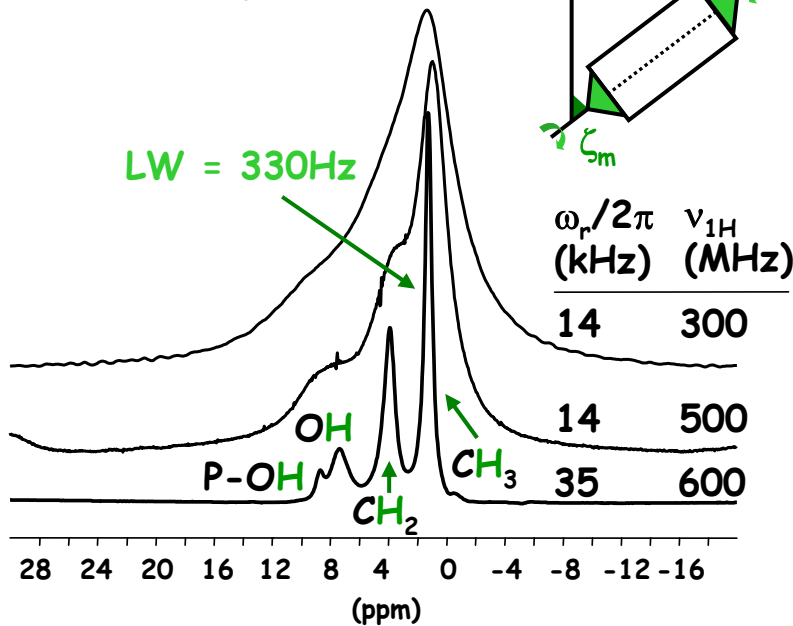
Exotic solid state NMR: ^1H and ^{35}Cl



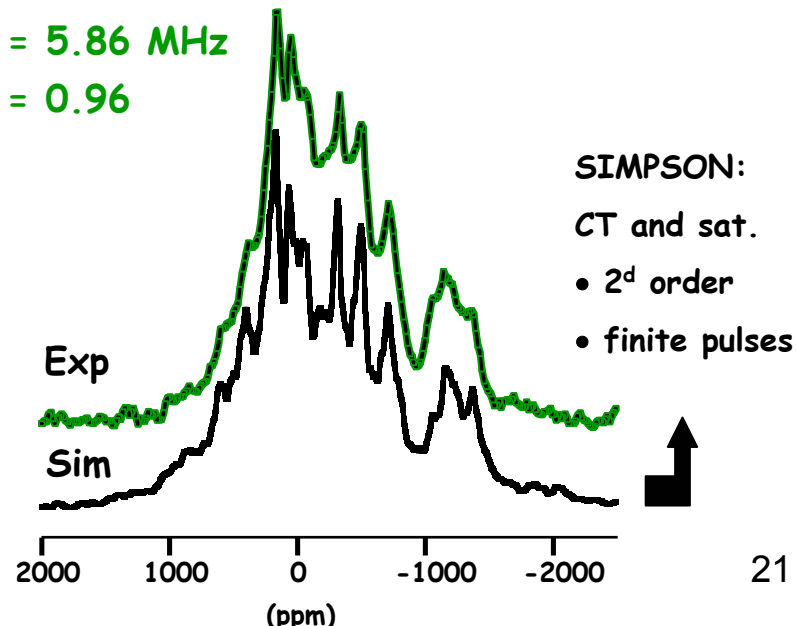
^1H 2.14 kHz
BR-24.....



LW = 330Hz



$C_Q = 5.86$ MHz
 $\eta_Q = 0.96$



Synthesis of zeolites: general approach

solution of silicates and aluminates
(high pH)

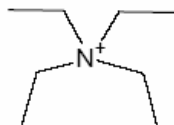
co-condensation: gel

templating agent

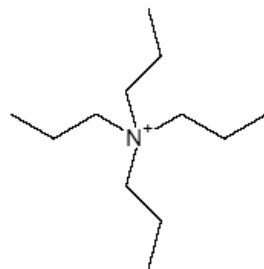
OH^- or F^-

hydrothermal condition
(T, P)

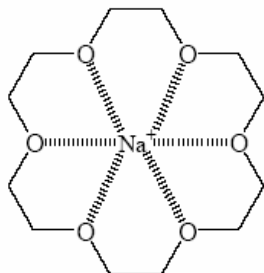
characterization (XRD..)



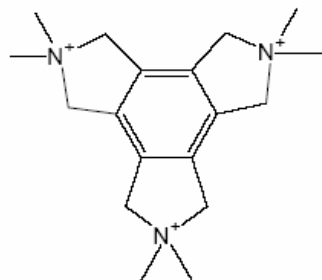
TEA⁺



TPA⁺



Na⁺ 18C6

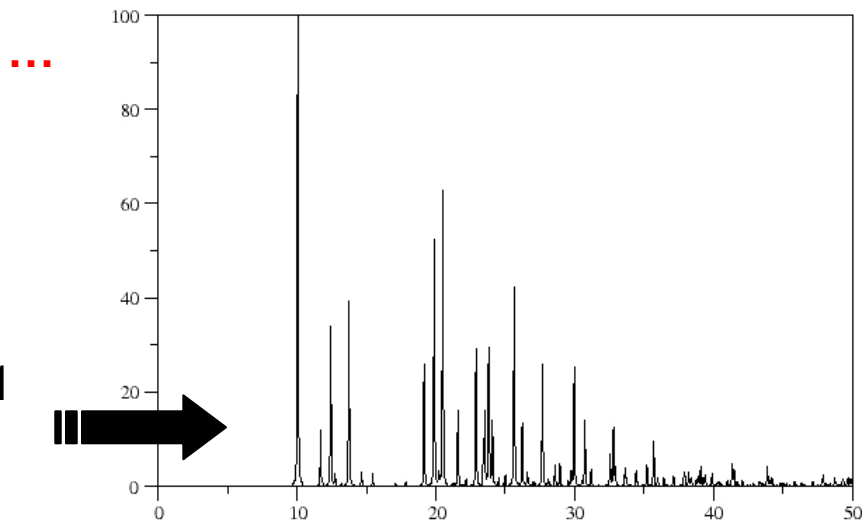


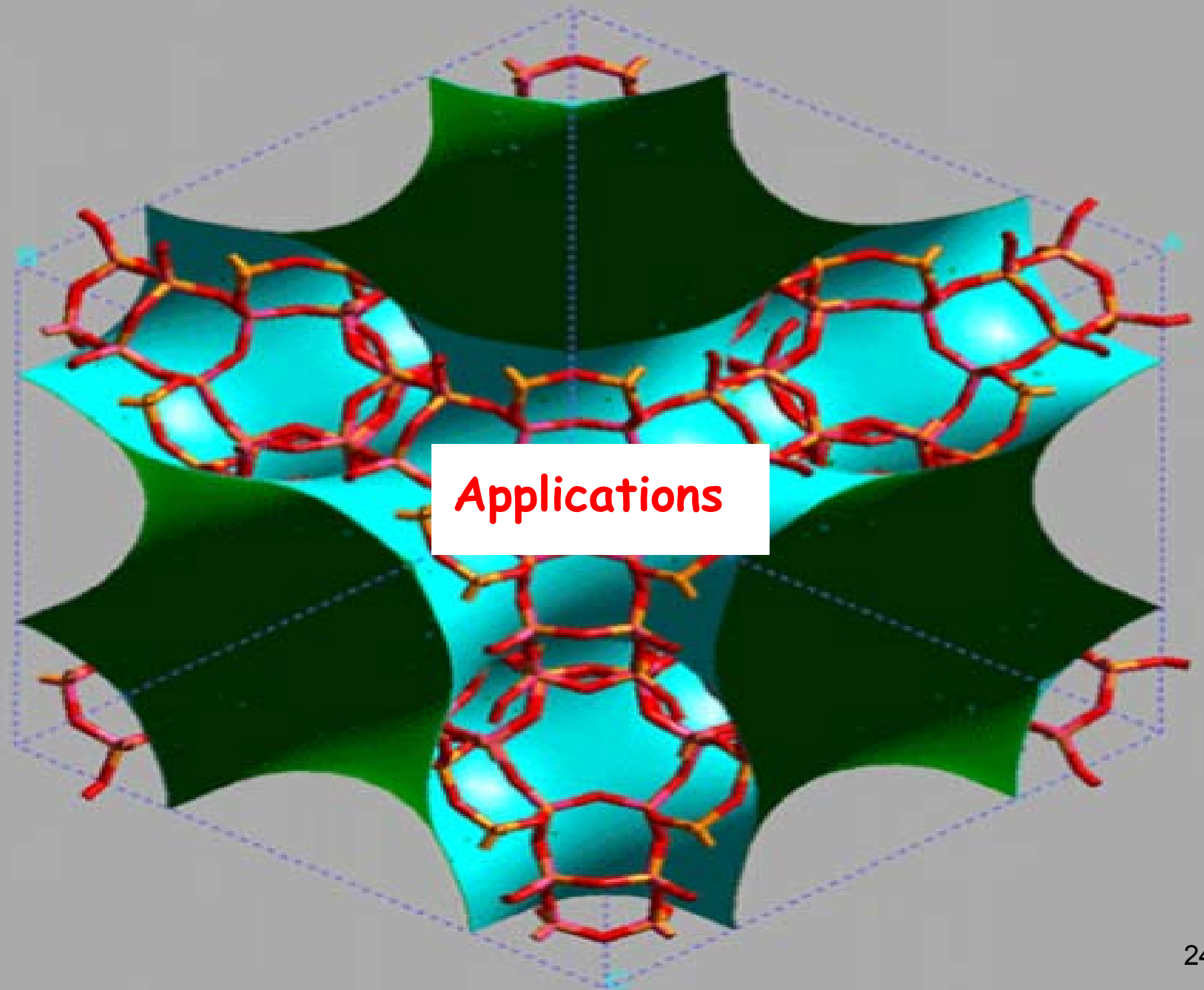
Welcome to the
Database of Zeolite Structures

- Atlas of Zeolite Framework Types
- Catalog of Disordered Zeolite Structures
- PDF Files of IZA Publications
- Collection of Simulated XRD
- Powder Patterns of Zeolites

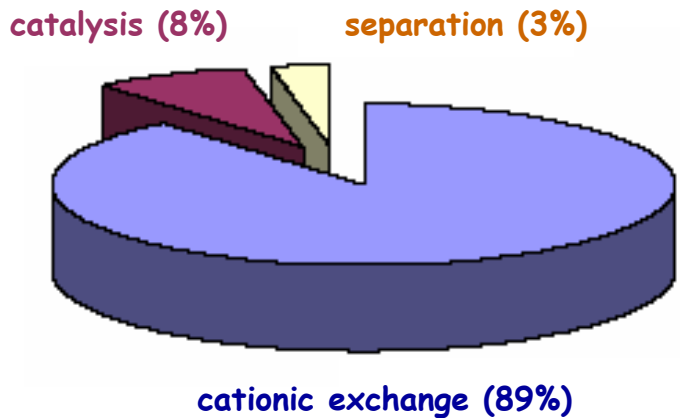


Tetramethylammonium ZAPO-M1
|N8C42.656| [Al25Zn7P32O128]

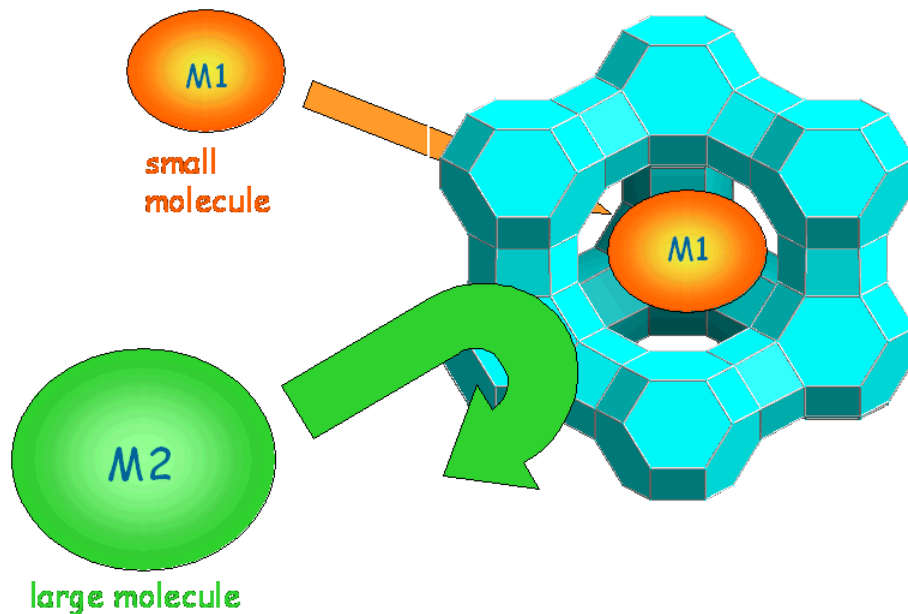




Molecular sieves

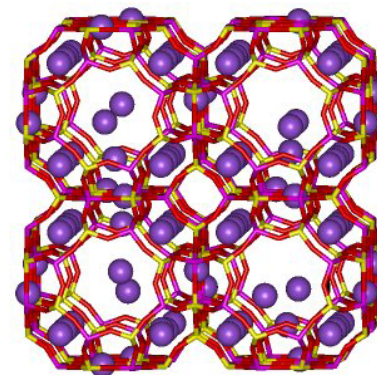
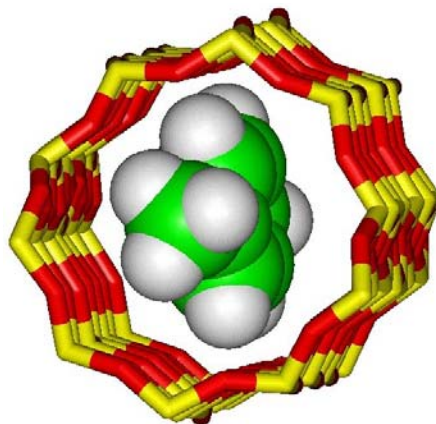


the concept...

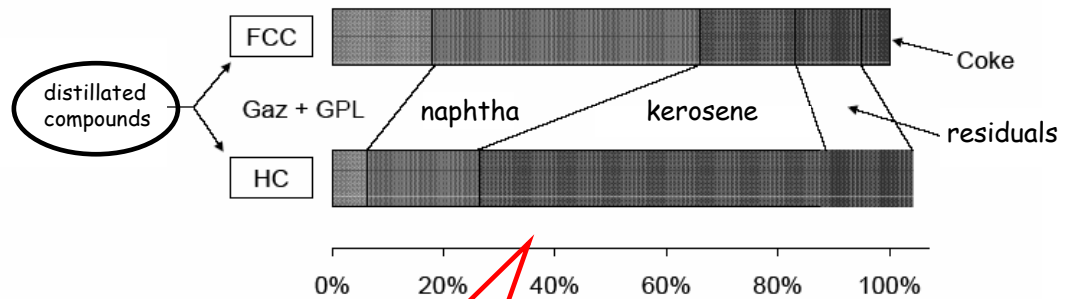
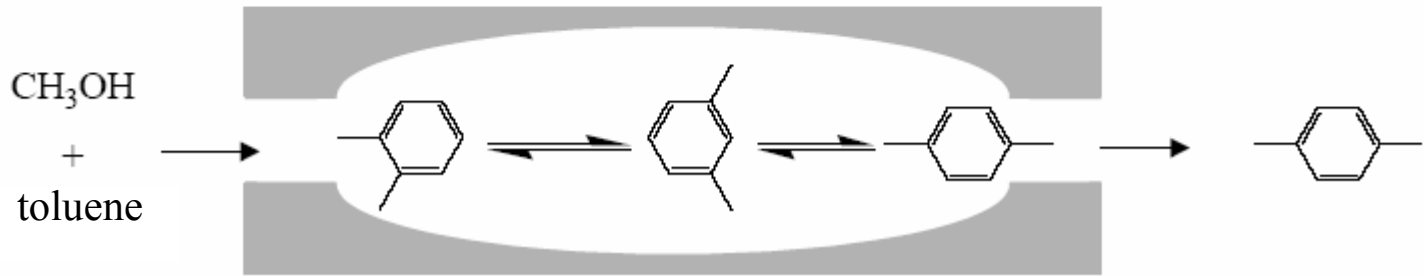


keywords:

- adsorption
- ion or molecule exchange
- substances removal
- catalysis



Catalysis



zeolite Y

Characterizing Zeolite Acidity by Spectroscopic and Catalytic Means: A Comparison[†]

S. Kotrel,^{‡,§} J. H. Lunsford,[§] and H. Knözinger^{*,‡}

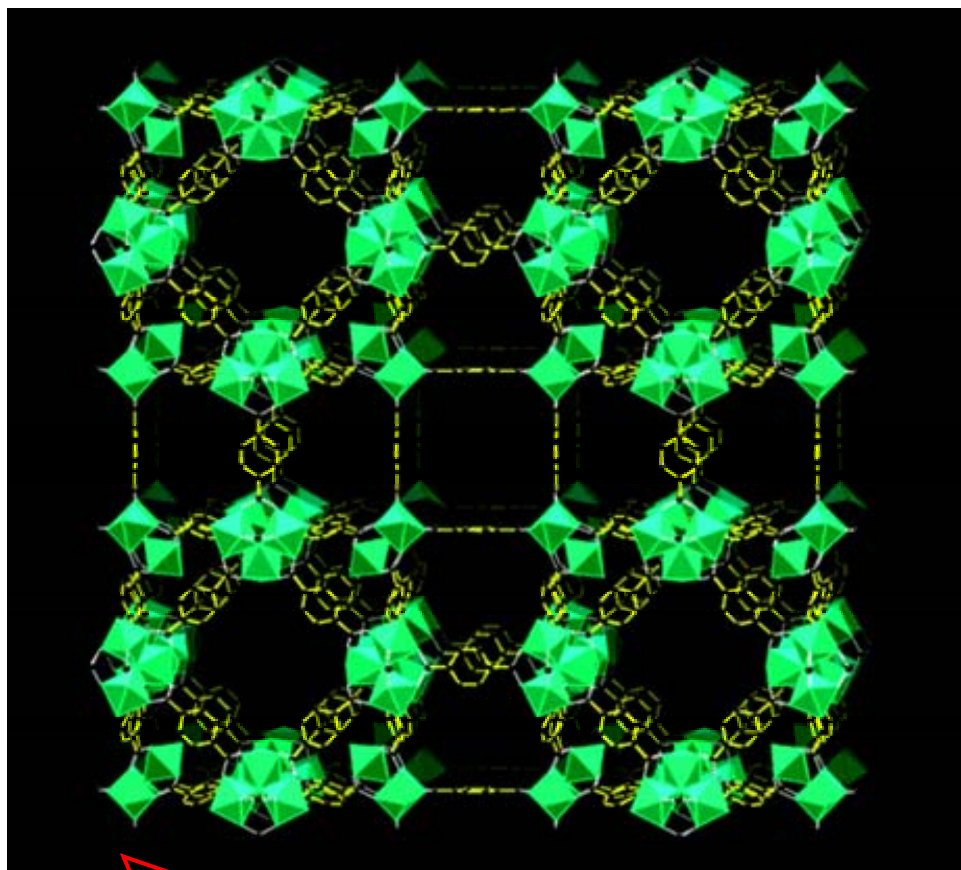
Department Chemie, Physikalische Chemie, LMU München, Butenandtstrasse 5-13 (Haus E); 81377 München, Germany, and Texas A & M University, Department of Chemistry, P.O. Box 30012, College Station, Texas 77842-3012

Received: June 16, 2000; In Final Form: October 27, 2000

Adsorption of H₂, N₂, and CO on four different protonated zeolites—H-ZSM-5, H-β, H-Y, and dealuminated H-Y—at low temperatures was studied by transmission Fourier transform infrared spectroscopy. The introduction of the basic probe molecules caused a red-shift of the IR stretching bands of the zeolitic acidic OH groups. This perturbation, which is commonly interpreted as a hydrogen bonding between the acidic OH group and the adsorbate and often taken as a measure of the acidic strength, was then compared with intrinsic activities for the acid-catalyzed cracking of *n*-hexane previously published for the same zeolite samples. Catalytic and spectroscopic characterization of the acidity is consistent only within the same class of zeolites, e.g. comparison of differently pretreated faujasites. Spectroscopic and catalytic observations for different types of zeolites do not match perfectly, because additional effects, such as interactions of larger molecules with pore walls and the stabilization of transition states and intermediates, can influence the course of an acid-catalyzed reaction.

Metal Organic Frameworks (MOFs)

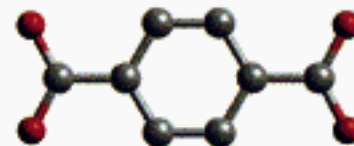
porous hybrid organic/inorganic solids



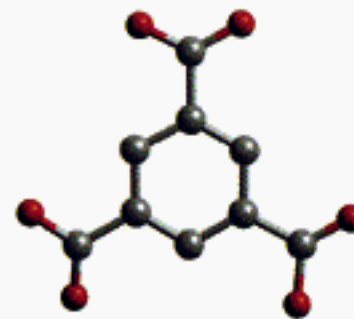
inorganic SBU's linked by organic bridges

O. M. Yaghi, G. Férey (~ 2000)

some organic ligands...

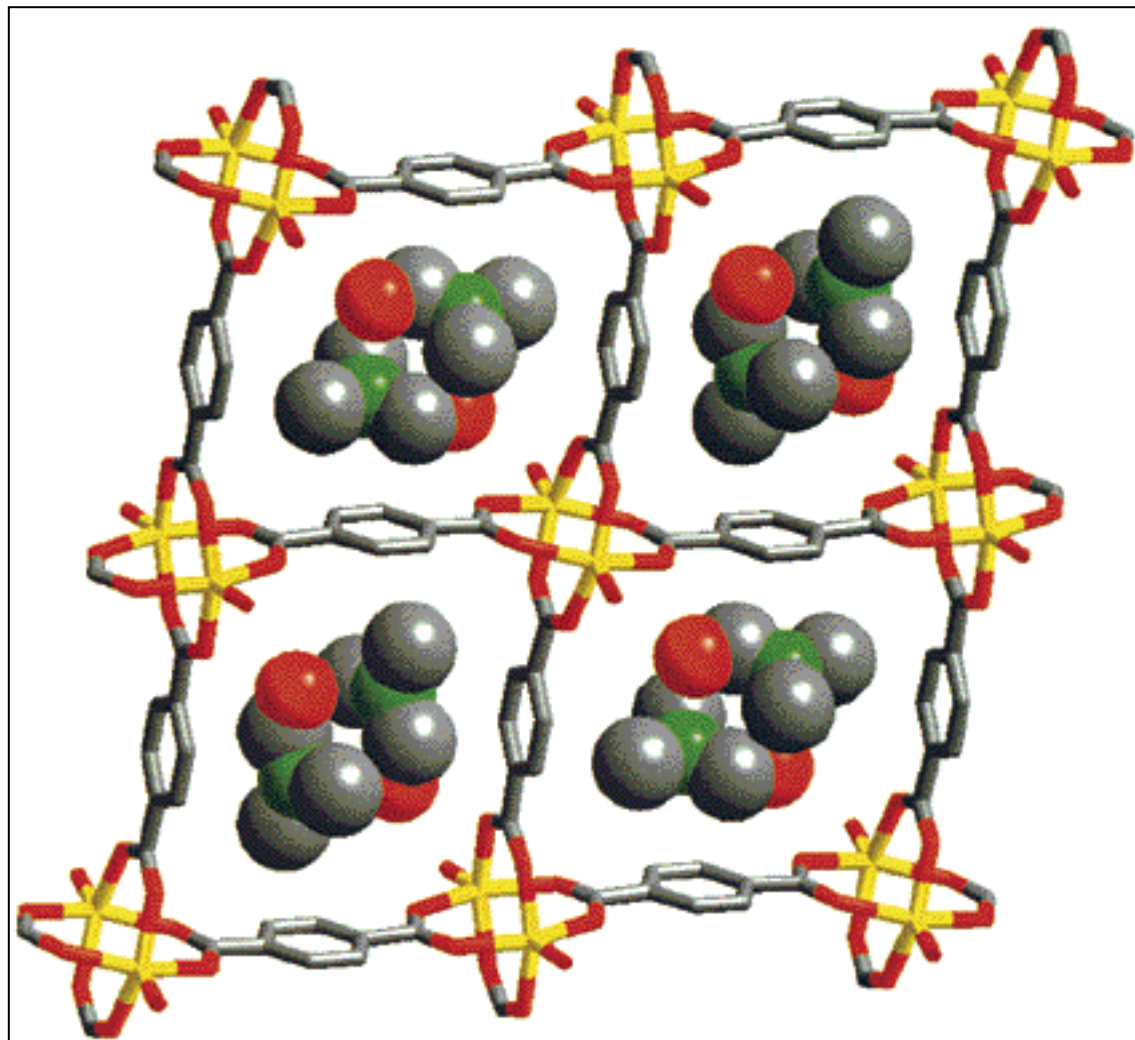
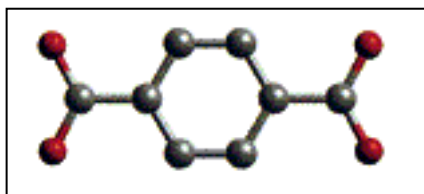
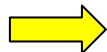
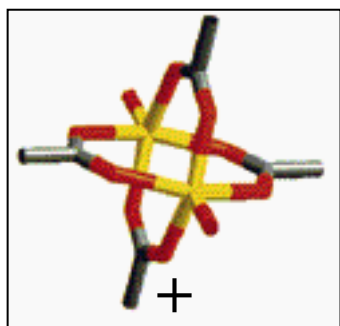
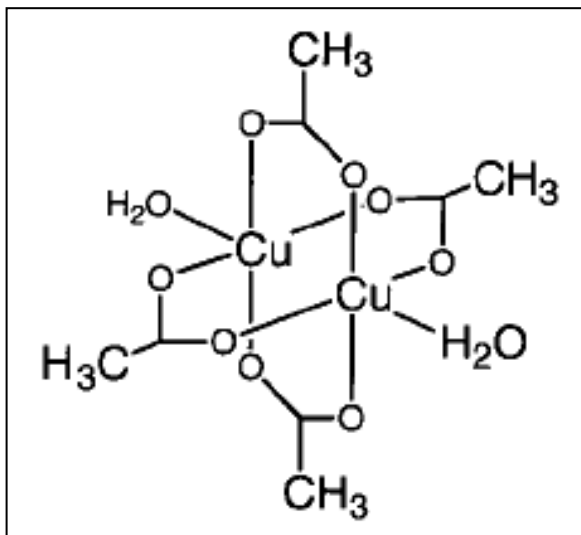


1,4-benzenedicarboxylate
(BDC)

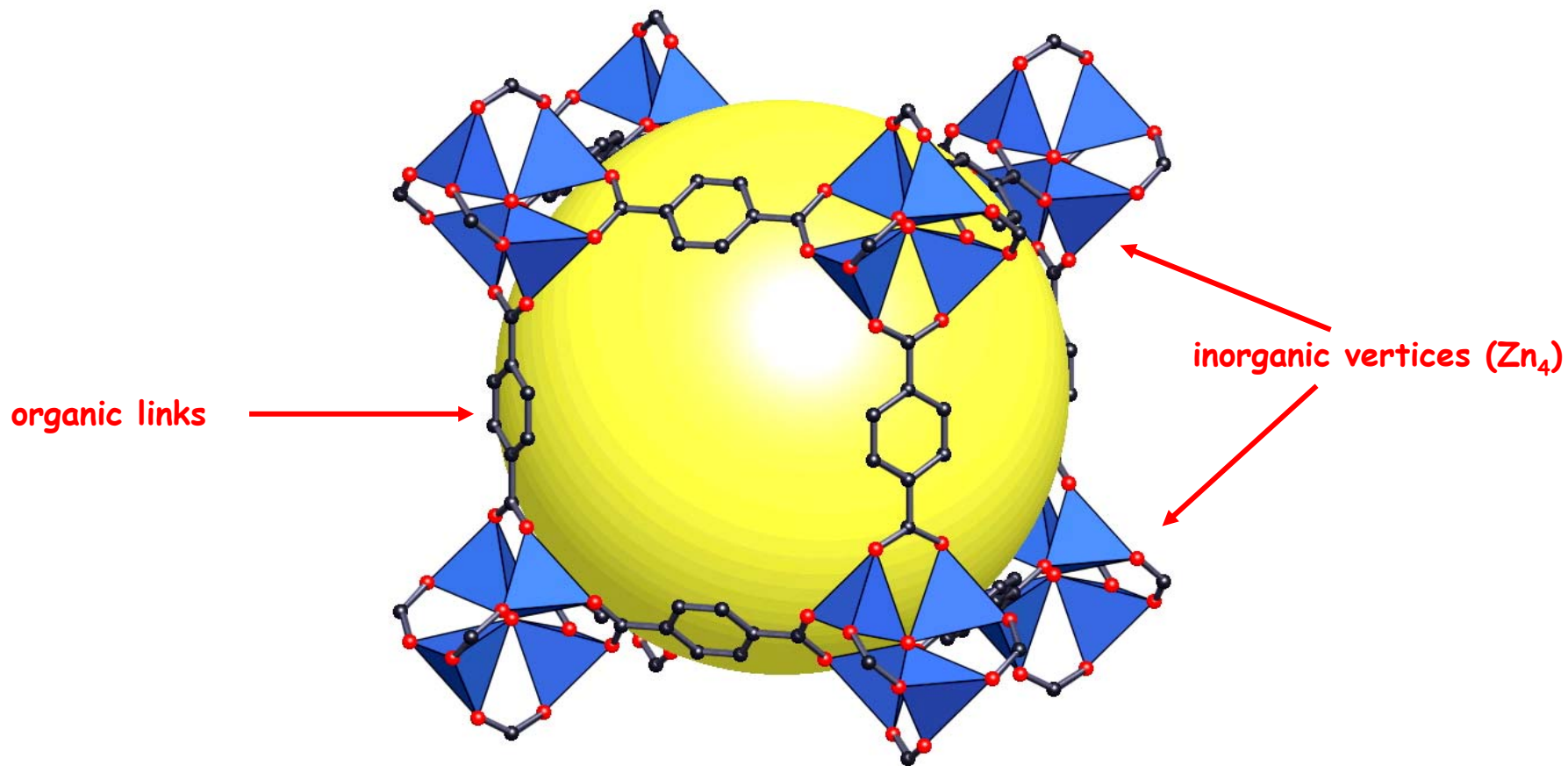


1,3,5-benzenetricarboxylate
(BTC)

An example



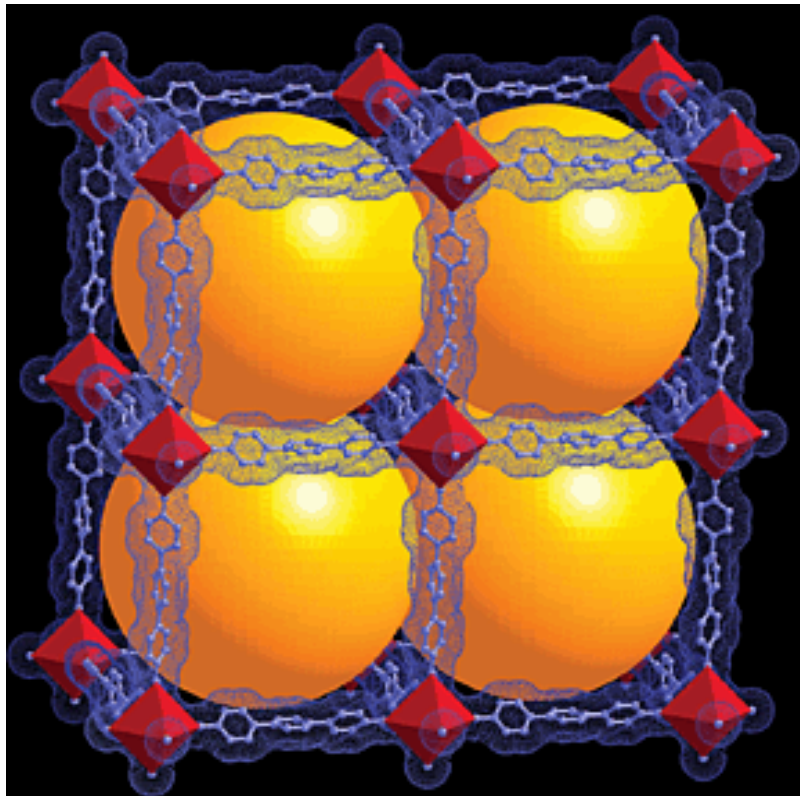
Crystal «sponges» - MOF-5



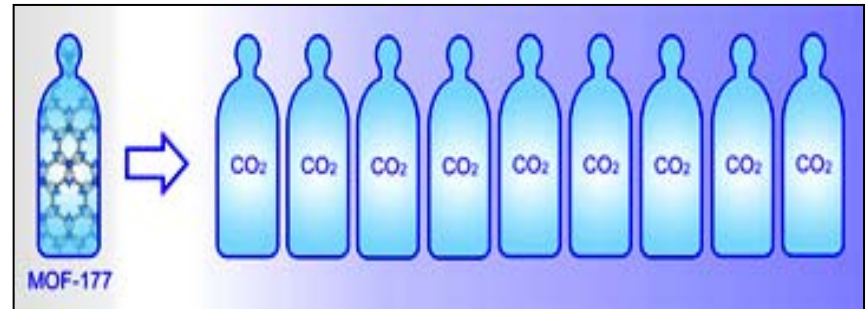
$d \sim 20 \text{ \AA}$

$S \sim 3000 \text{ m}^2 \cdot \text{g}^{-1} (?)$

cell $> 700.000 \text{ \AA}^3$



MOF-177



1 container with MOF-177 ~ 9 empty containers

other applications...

◇ drug delivery

◇ magnetic properties

◇ rare earths and luminescence...



The image is a transmission electron micrograph (TEM) of a mesoporous material. It displays a large, circular field of view filled with a highly ordered, periodic array of small, dark, spherical particles. These particles are arranged in a hexagonal lattice, with each particle surrounded by six neighbors. The particles are interconnected, forming a porous network. In the center of the image, there is a white rectangular box containing the text "Mesoporous materials" in red. Four white rectangular boxes are placed around the main image, each pointing to a corresponding inset image. The top-left inset shows a close-up of the hexagonal lattice. The top-right inset shows a different view of the lattice, possibly a different orientation. The bottom-left inset shows a close-up of the lattice with a white arrow pointing to the right. The bottom-right inset shows a close-up of the lattice with a white arrow pointing to the left. In the bottom right corner of the main image, there is a scale bar labeled "40 nm".

Mesoporous materials

40 nm

porous materials

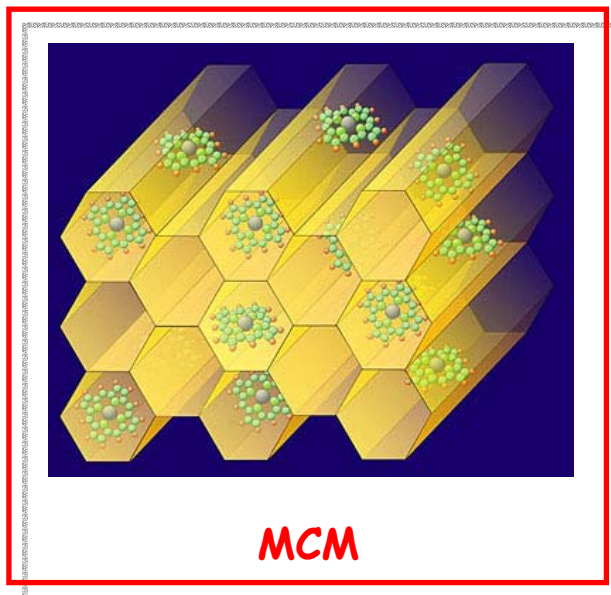
nanoporous
 $\varnothing < 2 \text{ nm}$

mesoporous
 $2 < \varnothing < 50 \text{ nm}$

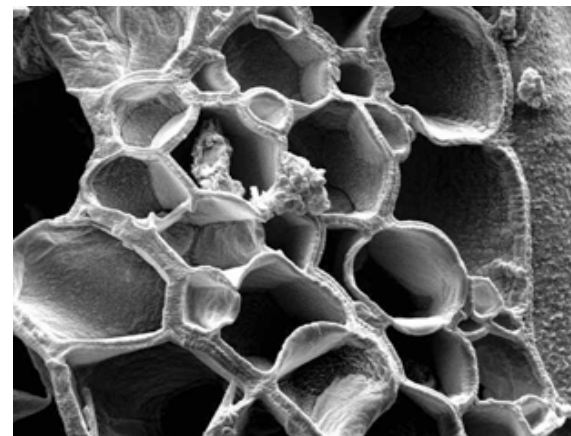
macroporous
 $50 \text{ nm} < \varnothing$



zeolites



MCM



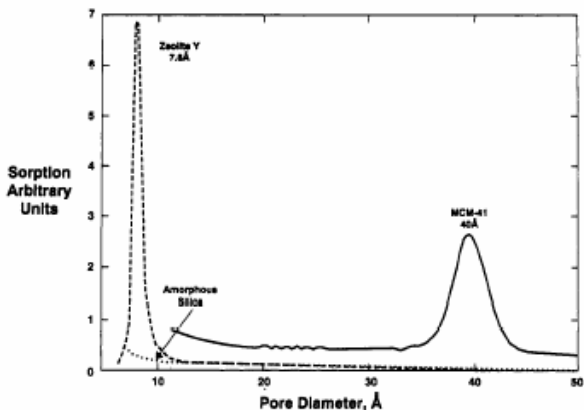
foams

1992: «the» breakthrough!

A New Family of Mesoporous Molecular Sieves Prepared with Liquid Crystal Templates

J. S. Beck,^{*,†} J. C. Vartuli,^{*,†} W. J. Roth,^{*,†} M. E. Leonowicz,^{*,†} C. T. Kresge,^{*,†}
K. D. Schmitt,[†] C. T-W. Chu,[†] D. H. Olson,[†] E. W. Sheppard,[†] S. B. McCullen,[†]
J. B. Higgins,[†] and J. L. Schlenker[†]

Contribution from the Mobil Research and Development Corporation, Central Research Laboratory, Princeton, New Jersey 08543, and Paulsboro Research Laboratory, Paulsboro, New Jersey 08066. Received June 30, 1992



Abstract: The synthesis, characterization, and proposed mechanism of formation of a new family of silicate/aluminosilicate mesoporous molecular sieves designated as M41S is described. MCM-41, one member of this family, exhibits a hexagonal arrangement of uniform mesopores whose dimensions may be engineered in the range of ~ 15 Å to greater than 100 Å. Other members of this family, including a material exhibiting cubic symmetry, have been synthesized. The larger pore M41S materials typically have surface areas above $700 \text{ m}^2/\text{g}$ and hydrocarbon sorption capacities of 0.7 cc/g and greater. A templating mechanism (liquid crystal templating—LCT) in which surfactant liquid crystal structures serve as organic templates is proposed for the formation of these materials. In support of this templating mechanism, it was demonstrated that the structure and pore dimensions of MCM-41 materials are intimately linked to the properties of the surfactant, including surfactant chain length and solution chemistry. The presence of variable pore size MCM-41, cubic material, and other phases indicates that M41S is an extensive family of materials.

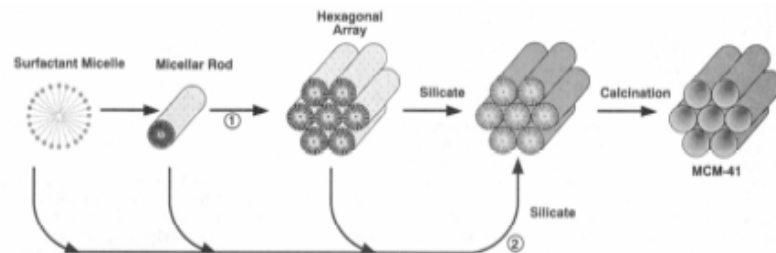
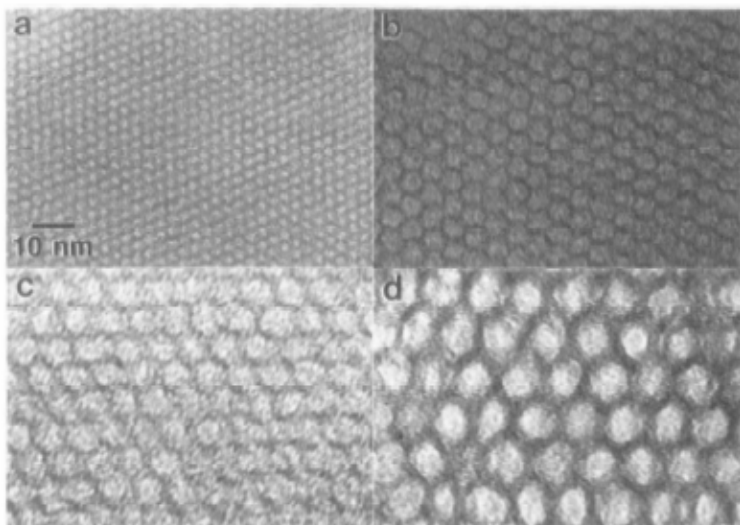


Figure 14. Possible mechanistic pathways for the formation of MCM-41: (1) liquid crystal phase initiated and (2) silicate anion initiated.

citations: 5367!

Pluronic® P123 Block Copolymer Surfactant

BASF

Langmuir 2005, 21, 431–436

Towerlike SBA-15: Base and (10)-Specific Coalescence of a Silicate-Encased Hexagonal Mesophase Tailored by Nonionic Triblock Copolymers

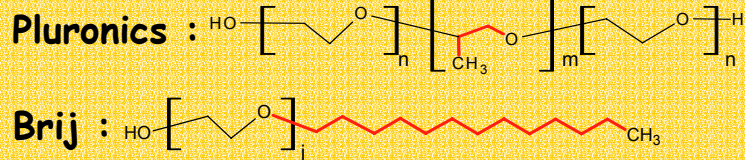
Yauh-Yarnng Fahn

Department of Chemical Engineering, Tung-Fang Institute of Technology, Hu-Nei, Kaohsiung 829, Taiwan

An-Chung Su and Pouyan Shen*

Institute of Materials Science and Engineering, National Sun Yat-sen University, Kaohsiung 804, Taiwan

Received November 24, 2003. In Final Form: August 8, 2004



Towerlike SBA-15

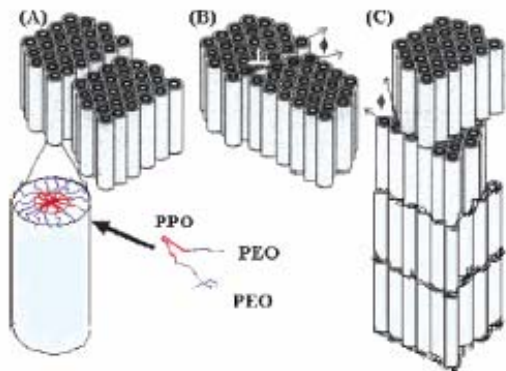


Figure 8. Proposed model for the hydrothermal mixing of $\text{EO}_{20}/\text{PO}_{70}/\text{EO}_{20}$ and TEOS under optimized HCl dosage: (A) original hexagonal column particulates with silicatropic rodlike micelles of $\text{EO}_{20}/\text{PO}_{70}/\text{EO}_{20}$ inset; (B) (10)-specific yet imperfect impingement of the column to form edge dislocations at the interface; (C) imperfect base attachment to form faulting with tubules offset and dislocations decorated at the suture zone.

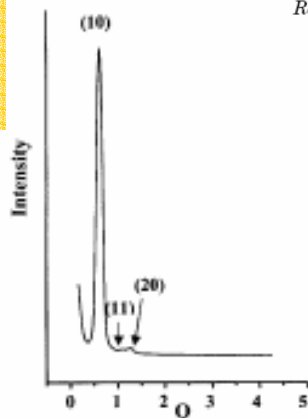


Figure 1. Small-angle X-ray scattering trace of the SBA-15 sample prepared by reacting $\text{EO}_{20}/\text{PO}_{70}/\text{EO}_{20}$ and TEOS under an optimized 2M HCl dosage (pH = 0.3) at 35 °C for 24 h followed by overnight aging at 80 °C and then template removal using ethanol. The (10), (11), and (20) peaks of 2-D hexagonal structure ($a = 11.73$ nm, with corresponding d spacing values of 10.16, 5.86, and 5.08 nm, respectively) were indexed according to a 2-D plane group scheme. The abscissa $Q = 2\pi/d$ is in inverted nanometers.

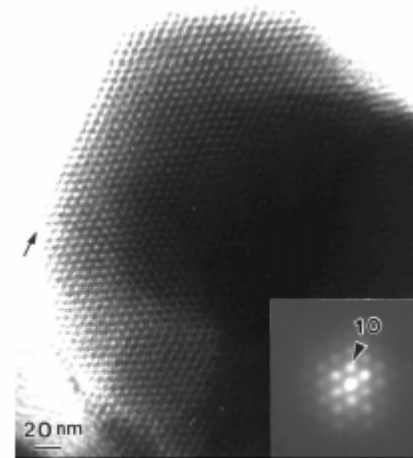
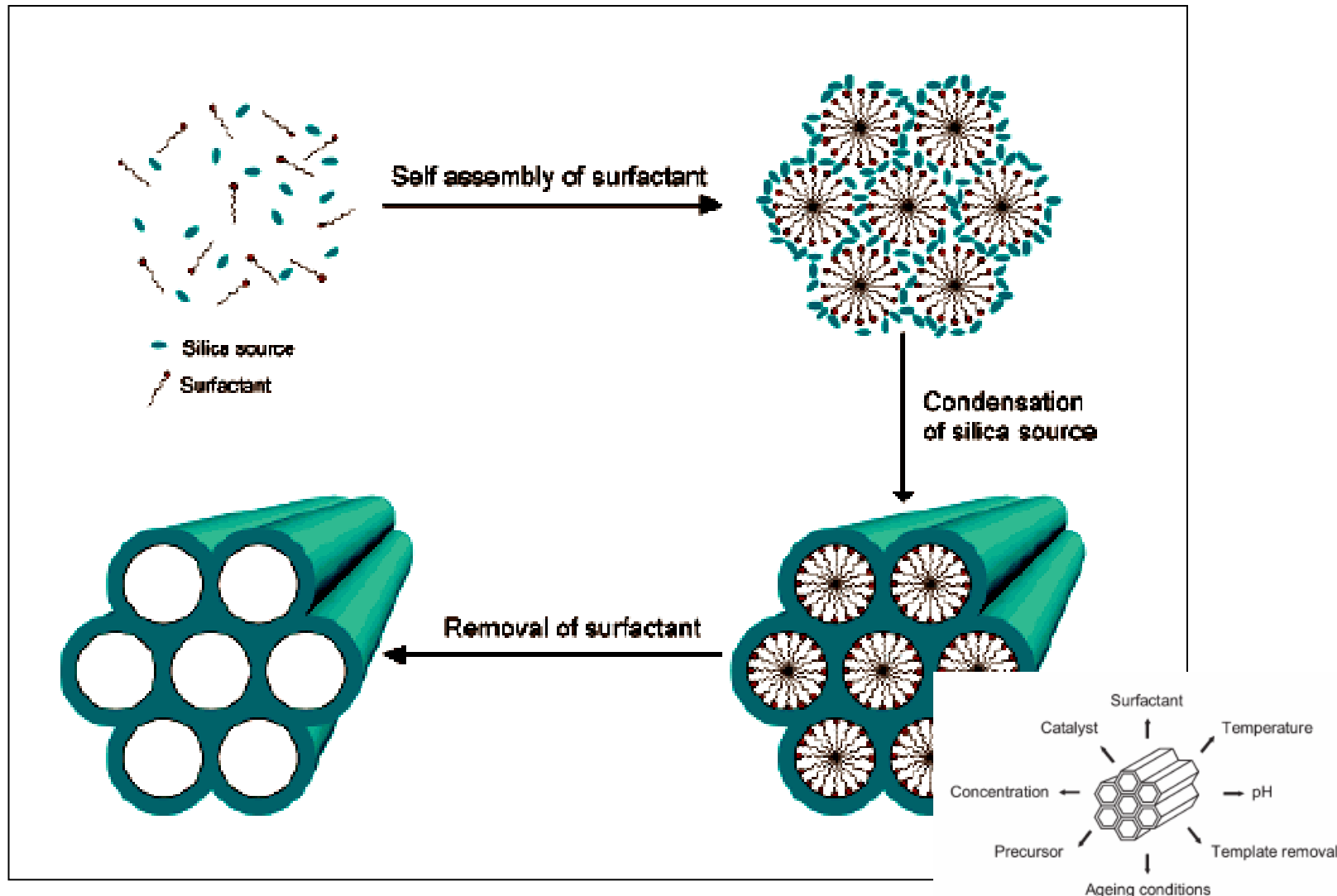
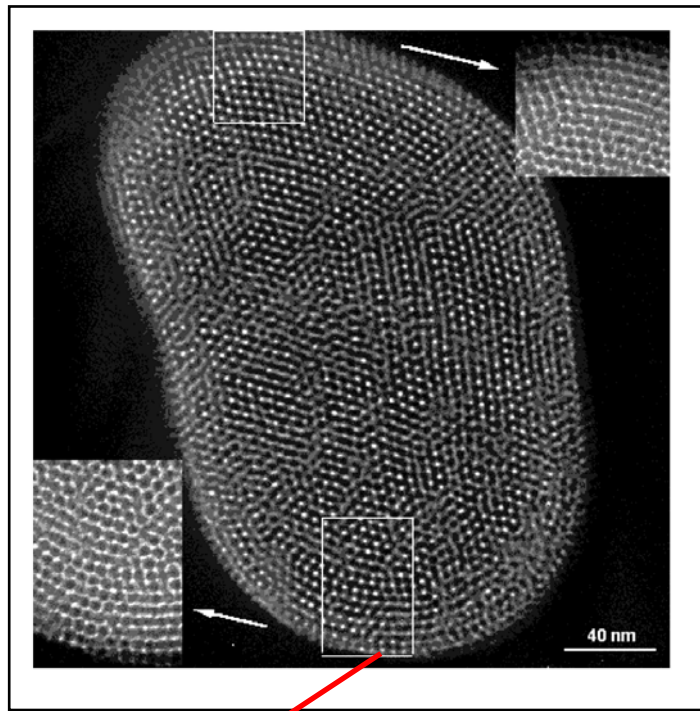


Figure 3. TEM photograph with an inset electron diffraction pattern of platelike SBA-15 hexagons (top view) showing a defect-free single domain with a well-developed (10) surface more or less with steps and a curved micelle wall (arrow). Note the hexagon has a rather flat base for uniform diffraction contrast.

Mesoporous materials



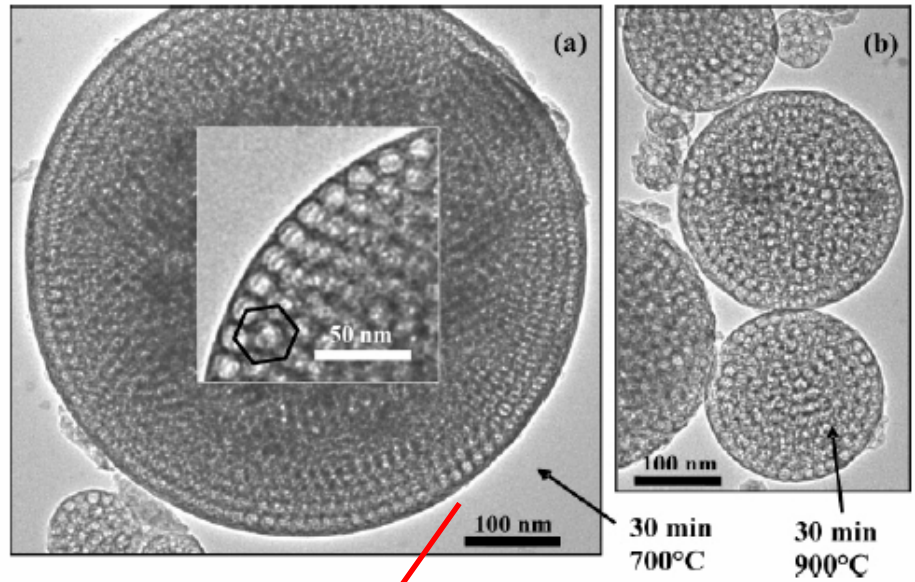
Mesoporous silica and other oxides



SiO_2

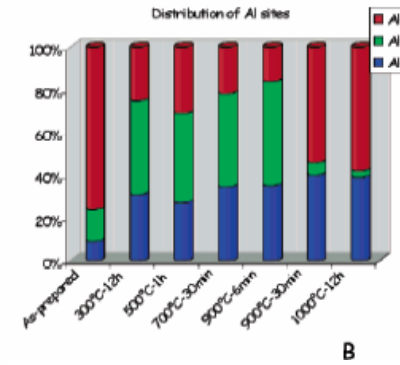
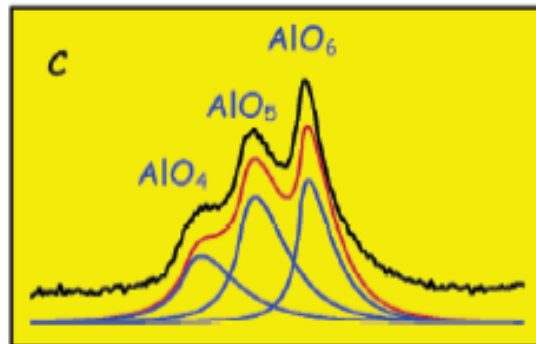
hydrolysis of TEOS

ordered network of pores
pores from 2 to 50 nm



Al_2O_3

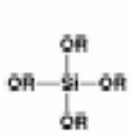
Boissière, Chem. Mater., 2006



Applications

towards a new chemistry...

pre-functionalisation



functional alkoxide

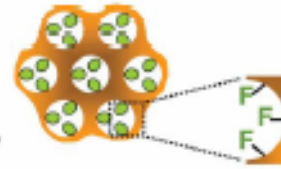


template (surfactant)

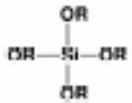


mesophase formation

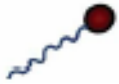
template removal



post-functionalisation



mesophase formation
template removal



functional group



grafting group

◇ organic functionalized silicas

◇ thin films

◇ surface grafting

◇ polymer hybrids

◇ nanocasting

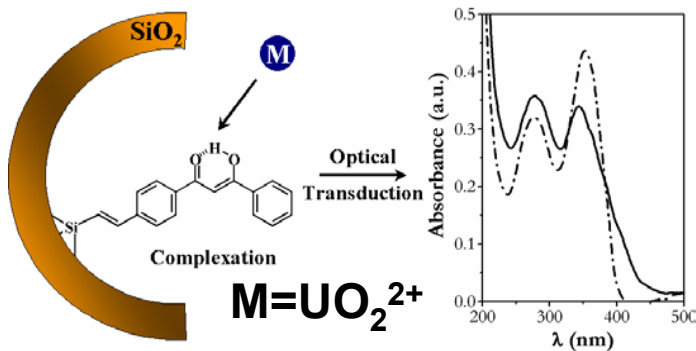
◇ bioencapsulation

◇ adsorption applications

◇ sensors, photoresponse

◇ ...

L. Nicole, J. Mater. Chem., 2005



sensors with optical detection

Solid-State NMR Study of Ibuprofen Confined in MCM-41 Material

Thierry Azaïs,^{*,†} Corine Tourné-Péteilh,[‡] Fabien Aussenac,[§] Niki Baccile,[†] Cristina Coelho,[†]
Jean-Marie Devoisselle,^{*,‡} and Florence Babonneau[†]

Université Pierre et Marie Curie—Paris 6, UMR 7574, Laboratoire Chimie de la Matière Condensée de Paris, Paris F-75005, France, Laboratoire de Matériaux Catalytiques et Catalyse en Chimie Organique, UMR 5618/ENSCM/Université Montpellier 1, 8 rue de l'École Normale, 34296 Montpellier Cedex 5, France, and Bruker Biospin, 34 rue de l'industrie, 67166 Wissembourg, France

Received July 5, 2006. Revised Manuscript Received October 20, 2006

Ibuprofen (an anti-inflammatory drug that is a crystalline solid at ambient temperature) has been encapsulated in MCM-41 silica matrices with different pore diameters (35 and 116 Å). Its behavior has been investigated by magic angle spinning (MAS) ^1H , ^{13}C , and ^{29}Si solid-state NMR spectroscopy at ambient and low temperature. This study reveals an original physical state of the drug in such materials. At ambient temperature, ibuprofen is not in a solid state (crystalline or amorphous) and is extremely mobile inside the pores, with higher mobility in the largest pores (116 Å). The interaction between ibuprofen and the silica surface is weak, which favors fast drug release from this material in a simulated intestinal or gastric fluid. The quasi-liquid behavior of ibuprofen allows the use of NMR pulse sequences issued from solution-state NMR, such as the INEPT sequence, to characterize these solid-state samples. The solid-state MAS NMR study shows that the proton of the carboxylic acid group of ibuprofen is in a chemical exchange at ambient temperature. Furthermore, at low temperature (down to 223 K), NMR spectroscopy results show that ibuprofen is able to crystallize inside the largest pores (116 Å), whereas a glassy state is obtained for the smallest ones (35 Å).

